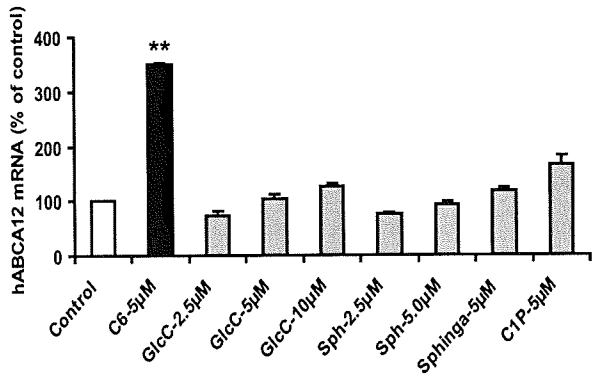

FIGURE 2. **Exogenous ceramide stimulates ABCA12 mRNA.** Primary cultured human keratinocytes were incubated in the presence or absence of C_6-Cer, glucosylceramide (*GlcC*), sphingosine (*Sph*), sphinganine (*Sphinga*), or ceramide 1-phosphate (*C1P*) for 16 h. ABCA12 and cyclophilin mRNA levels were then measured as described under "Experimental Procedures." Data are expressed as a percentage of control (100%) and presented as mean ± S.E. (n = 3–4). Similar results were obtained when the experiment was repeated with a different batch of cells. **, $p < 0.01$; C: C_6-Cer.

PPARδ siRNA (ON-TARGETplus SMARTpool) was purchased from Dharmacon, Inc. For human alkaline ceramidase 1 siRNA, cultured human keratinocytes were transfected at a concentration of 10 nM using Lipofectamine and PLUS reagents (Invitrogen) according to the manufacturer's instructions. For human PPARδ siRNA, cultured human keratinocytes were transfected at a concentration of 30 nM using SiLentFect™ Lipid (Bio-Rad), followed by 24-h treatment with C_6-Cer. Cells were then harvested and subjected to mRNA measurement by reverse transcription-quantitative PCR.

Western Blot Analysis—Western blots were carried out according to the manufacturer's protocol. Briefly, for ABCA12, 80–100 μg of proteins prepared from keratinocytes were fractionated on precast gels (3–8%) and transferred to polyvinylidene difluoride membranes overnight at 4 °C. The proteins on the membrane were subsequently probed with monoclonal primary antibodies against human ABCA12 (30) and then visualized by secondary antibody using the ECL Western blotting detection system kit. Membranes were then exposed to CL-XPosure film. For PPARδ, similar procedures were used, except following treatment, nuclear proteins were prepared from keratinocytes, as described previously (31). An identical blot was probed with anti-β-actin antibody to verify the equal loading of protein.

Lipid Analysis—The endogenous ceramide levels in the total cellular lysates were measured as described previously (32). Lipid extracts were prepared from cellular homogenates by the method of Bligh and Dyer (33). Separation of individual lipid species was achieved by HPTLC, followed by quantification by scanning densitometry (32). Glucosylceramides and ceramides were separated first using chloroform/methanol/water (40:10:1, v/v/v) to 2.0 cm and to 5.0 cm and then chloroform/methanol/acetic acid (94:4:1, v/v/v) to 8.5 cm, followed by *n*-hexane-diethyl acetic acid (65:35:1, v/v/v) to the top of the plate.

Statistical Analysis—All data are expressed as mean ± S.E., except for ceramide quantification, which is expressed as mean ± S.D. Comparison between two groups is undertaken using two-tail and unpaired t test. Differences in values are considered significant if p is <0.05.

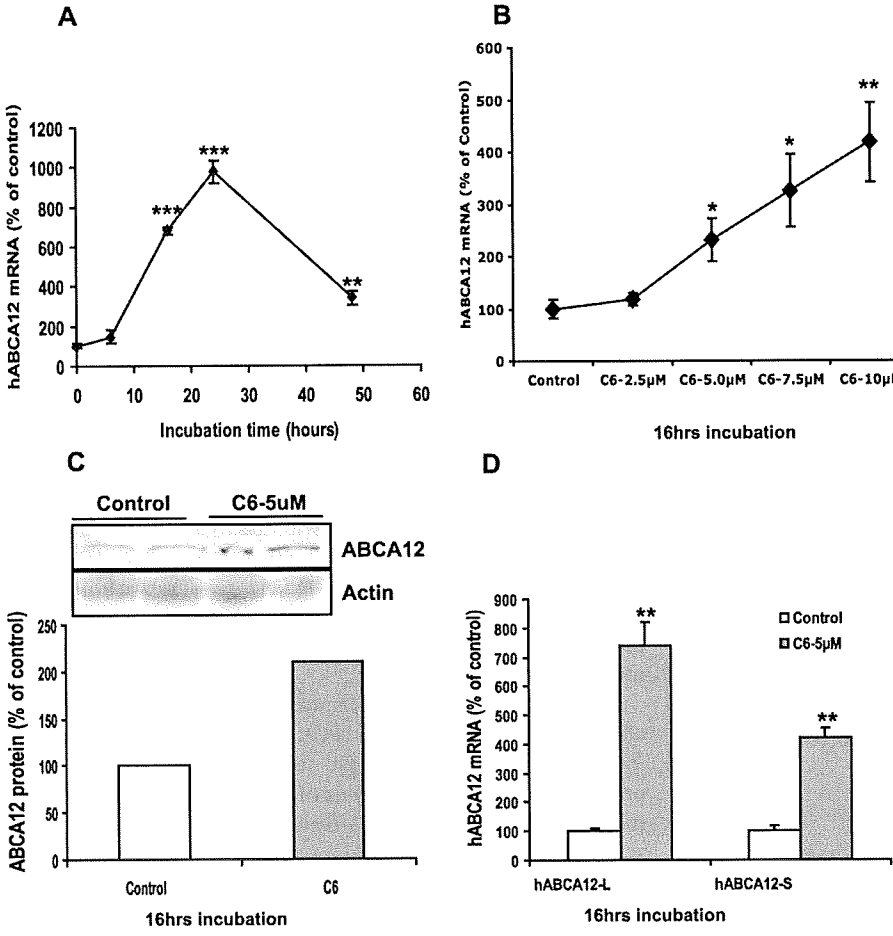

FIGURE 3. **Ceramide stimulates ABCA12 mRNA expression in a time- and dose-dependent manner.** Cultured human keratinocytes were incubated with C_6-Cer (5 μM) for various periods of time (0, 9, 16, 24, and 48 h) (*A*). Alternatively, cells were incubated with various doses of C_6-Cer (0–10 μM) for 16 h (*B*). Messenger RNA levels of full-length ABCA12 or cyclophilin were measured as described. Data are expressed as a percentage of vehicle control (100%) and presented as mean ± S.E. (n = 3–5). *C*, ABCA12 and β-actin protein levels were measured by Western blot following C_6-Cer treatment for 16 h. Similar results were obtained when the experiment was repeated with a different batch of cells. *D*, messenger RNA levels of ABCA12 variants (ABCA12-L and -S) were measured, expressed as a percentage of vehicle control (100%), and presented as mean ± S.E. (n = 4). *, $p < 0.05$; **, $p < 0.01$; ***, $p < 0.001$; C: C_6-Cer.

RESULTS

Exogenous Ceramides but Not Other Sphingolipids Stimulate ABCA12 mRNA—To determine whether sphingolipids regulate

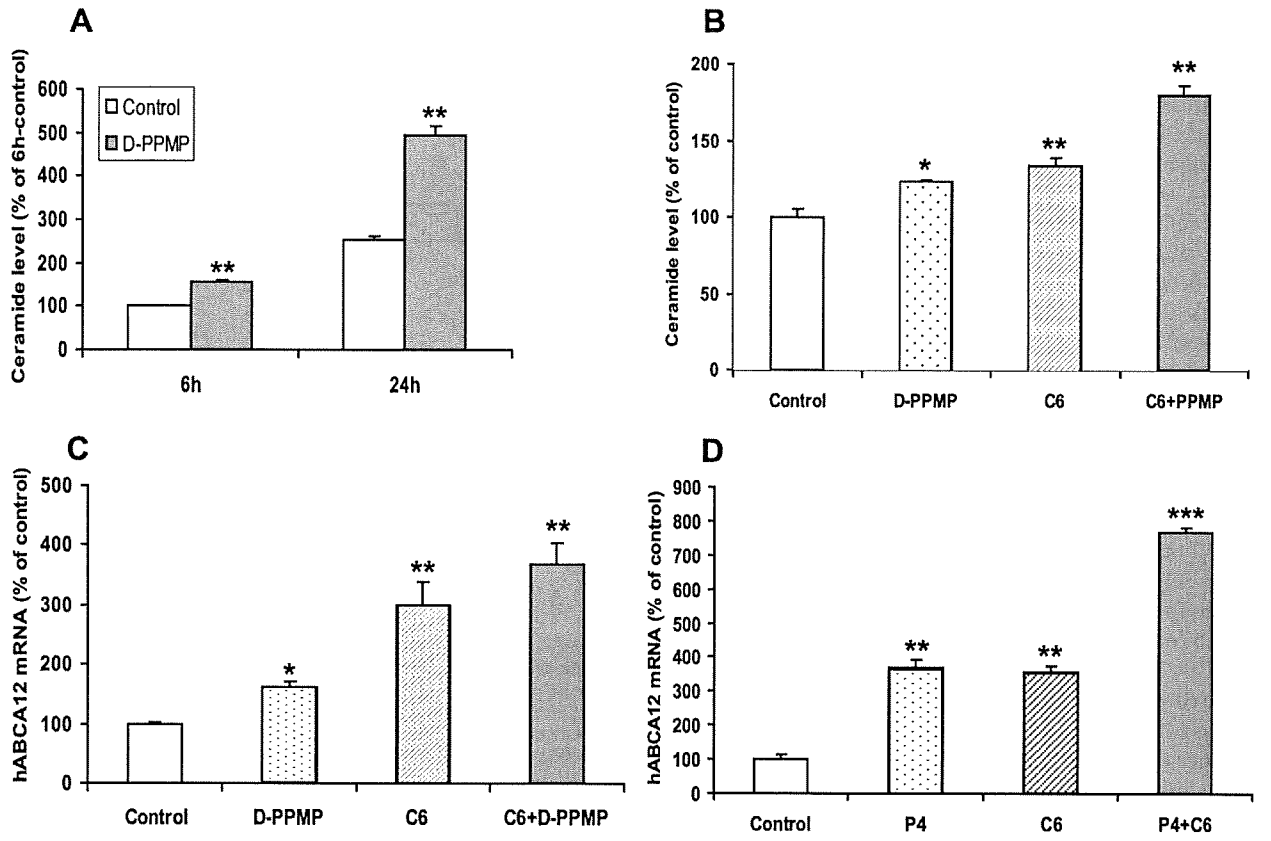

FIGURE 4. **Glucosyltransferase inhibitors increase endogenous ceramide levels and induce ABCA12 mRNA.** *A*, cultured human keratinocytes were incubated with vehicle control (*open bars*) or D-PPMP (10 μM; *solid bars*) for 6 or 24 h, and ceramide levels were determined as described under "Experimental Procedures." Data are expressed as mean ± S.D. ($n = 4$). *B*, cells were incubated with vehicle, D-PPMP (5 μM; *dotted bar*), C_6-Cer-5 μM (as positive control; *hatched bar*), or D-PPMP plus C_6-Cer (*solid bar*) for 16 h. *C*, ceramide levels were determined after cells were incubated with vehicle, D-PPMP, C_6-Cer, or D-PPMP plus C_6-Cer for 6 h. Another set of cells were incubated with vehicle, C_6-Cer (5 μM), P4 (10 μM), or P4 plus C_6-Cer for 16 h (*D*). ABCA12 mRNA levels (*B* and *D*) were measured as described. Data are expressed as a percentage of control (100%) and presented as mean ± S.D. ($n = 3$–4). Experiments were repeated at least once with similar results. *, $p < 0.05$; **, $p < 0.01$; ***, $p < 0.001$; C6: C_6-Cer.

ABCA12 gene expression, we initially examined the effect of various exogenously added sphingolipids, including C_6-Cer, C_8-β-D-glucosyl ceramide, sphingosine, sphinganine, or ceramide 1-phosphate, on ABCA12 mRNA expression in cultured human keratinocytes (Fig. 2). C_6-Cer, a synthetic ceramide that is cell-permeable, increased ABCA12 mRNA levels ~3.5-fold. Similarly, another synthetic ceramide, C_2-Cer, also increased ABCA12 mRNA levels (data not shown). In contrast, neither synthetic C_8-β-D-glucosyl ceramide, sphingosine, sphinganine, nor ceramide 1-phosphate induces ABCA12 mRNA expression (Fig. 2). These results indicate that ceramides but not other major metabolites of ceramide elevate ABCA12 mRNA levels in human keratinocytes.

Ceramide Stimulates ABCA12 Expression in a Time- and Dose-dependent Manner—As shown in Fig. 3*A*, C_6-Cer increased ABCA12 mRNA levels in a time-dependent fashion, with a large increase first seen at 16 h and a further increase by 24 h, which was diminished at 48 h. Further, C_6-Cer also increased ABCA12 mRNA levels in a dose-dependent manner, with a half-maximal effect at 5 μM (Fig. 3*B*). Higher doses (≥12.5 μM) of C_6-Cer were toxic to the cells (data not shown). Interestingly, the stimulatory effect of C_6-Cer is specific for ABCA12, since C_6-Cer did not induce the expression of another ABC transporter, ABCA1 (data not shown). Similarly, C_2-Cer, another synthetic and cell-permeable ceramide, also increased ABCA12 mRNA in a similar dose- and time-dependent manner (data not shown). Furthermore, consistent with our mRNA data, an increase in ABCA12 protein mass (~2-fold) was evident following C_6-Cer treatment (Fig. 3*C*). Together, these results indicate that exogenous ceramide induces ABCA12 expression in cultured human keratinocytes.

Finally, we reported previously that two major splicing transcripts of ABCA12, ABCA12-L and -S, are expressed in cultured human keratinocytes and that both are up-regulated by PPAR and LXR activation (18). We therefore examined whether C_6-Cer also stimulates the expression of one or both of these transcripts. As we reported previously (18), the basal expression level of ABCA12-L mRNA is higher than ABCA12-S (C_T ~24 *versus* ~30). However, both transcripts are up-regulated by C_6-Cer treatment (7- and 4-fold, respectively) (Fig. 3*D*). Thus, like PPAR and LXR activators, C_6-Cer increases the expression of both ABCA12-L and -S transcripts in cultured human keratinocytes.

Glucosyltransferase Inhibitors Increase Endogenous Ceramide Levels and Induce ABCA12 Expression—To further elucidate the mechanism responsible for ceramide-induced

ABCA12 expression, we next examined ABCA12 mRNA levels after raising endogenous ceramide levels by inhibiting glucosylceramide synthase activity with three different inhibitors (Fig. 1). Treatment of cultured human keratinocytes with D-PPMP for a short (6 h) or long (24 h) period of time increased total intracellular ceramide levels (Fig. 4*A*) and decreased glucosylceramide levels by ~58% (data not shown). Pertinently, treatment of cells with D-PPMP also increased ABCA12 mRNA levels (Fig. 4*B*), and co-treatment with D-PPMP and exogenous C_6-Cer provoked a greater increase in ABCA12 mRNA level than was observed with either treatment alone, indicating an additive effect (Fig. 4*B*). Accordingly, although D-PPMP or C_6-Cer alone increases intracellular ceramide levels, the combination of D-PPMP and C_6-Cer results in a greater increase in ceramide levels (Fig. 4*C*), which could contribute to the greater increase in ABCA12 mRNA levels with combination treatment. Additionally, we also treated cells with P4, another inhibitor of glucosylceramide synthase, and observed a similar increase in ABCA12 mRNA levels and an additive effect with exogenous C_6-Cer (Fig. 4*D*). Furthermore, DL-*threo*-1-phenyl-2-decanoylamino-3-morpholino-1-propanol·HCl (DDMP), another inhibitor of glucosylceramide synthase, also increased ABCA12 mRNA levels (data not shown). These results indicate that the conversion of ceramide to glucosylceramide cannot be the basis for the C_6-Cer-induced increase in ABCA12 expression, since one would have expected a decrease rather than an additive induction with simultaneous treatment with glucosylceramide synthase inhibitors. Together, these data indicate that glucosylceramide synthase inhibitors increase endogenous ceramide levels and increase ABCA12 mRNA levels and also that the conversion of ceramide to glucosylceramide is not required for the stimulation of ABCA12 expression.

Sphingomyelin Synthase Inhibitors Increase Endogenous Ceramide Levels and Induce ABCA12 mRNA—In addition to glucosylceramides, ceramides can also be readily converted into sphingomyelin, a step that can be blocked with D609, a sphingomyelin synthase inhibitor (Fig. 1). Therefore, we initially quantified intracellular ceramide levels following D609 treatment, and as predicted, after a 6- or 24-h incubation, D609 increased ceramide levels (Fig. 5*A*). Moreover, incubation with D609 increased ABCA12 mRNA levels. However, the combination of D609 with exogenous C_6-Cer did not additively affect ABCA12 expression (Fig. 5*B*). Thus, increasing endogenous ceramide levels by inhibiting sphingomyelin synthase stimulates *ABCA12* gene expression, similar to our observations with glucosylceramide synthase inhibition noted above. Additionally, these results demonstrate that the conversion of C_6-Cer to sphingomyelin is not required for the ceramide-mediated increase in ABCA12 expression.

Ceramidase Inhibitors Increase Endogenous Ceramide Levels and Induce ABCA12 mRNA—In addition to serving as a substrate for the formation of complex sphingolipids (glucosylceramides and sphingomyelin), ceramides can be further hydrolyzed into sphingosine, catalyzed by a family of ceramidases (Fig. 1). Previously it has been reported that four of the five known ceramidase isoforms are widely expressed in cutaneous and extracutaneous tissues, including alkaline and acidic ceramidases (34), which can be blocked by D-MAPP and B13,

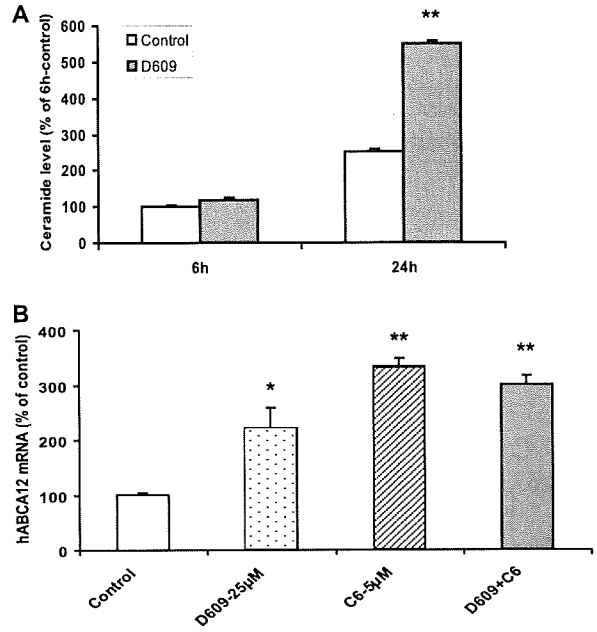

FIGURE 5. **Sphingomyelin synthase inhibitors increase endogenous ceramide levels and induce ABCA12 mRNA.** Cultured human keratinocytes were incubated with vehicle (*open bars*) or D-609 (25 μM; *solid bars*) for 6 or 24 h, and ceramide levels were determined ($n = 4$) (*A*). Alternatively, cells were incubated with vehicle, D609 (25 μM; *dotted bar*), C6–5 μM (*hatched bar*), or D609 plus C_6-Cer (*solid bar*) for 16 h. ABCA12 mRNA levels were measured as described (*B*). Data are expressed as a percentage of control (100%) and presented as mean ± S.E. ($n = 3$). Experiments were repeated at least once with similar results. *, $p < 0.05$; **, $p < 0.01$; C6: C_6-Cer.

respectively. Furthermore, as noted above, exogenous sphingosine failed to stimulate ABCA12 mRNA expression (Fig. 2).

D-MAPP, an alkaline ceramidase inhibitor, has been shown to increase endogenous ceramide levels in a cancer cell line (35). As expected, D-MAPP treatment increased intracellular ceramide levels in cultured human keratinocytes (Fig. 6*A*). Moreover, D-MAPP increases ABCA12 mRNA levels, and the combination with C_6-Cer was additive (Fig. 6*B*). In contrast, L-MAPP, a non-biological enantiomer of D-MAPP (35) that does not inhibit alkaline ceramidase activity, had no effect on *ABCA12* expression (data not shown). Additionally, when alkaline ceramidase-1 mRNA was knocked down by siRNA transfection, a 2-fold increase in ABCA12 mRNA levels was observed in transfected cells compared with controls (Fig. 6*C*).

B13, a compound that specifically inhibits cellular acidic ceramidase activity (36), resulting in the intracellular accumulation of ceramide (37), also induces ABCA12 mRNA levels and is additive to the effects of C_6-Cer (Fig. 6*D*). Finally, whereas suboptimal concentrations of either D-MAPP or B13 only slightly increase ABCA12 mRNA levels, the combination of these two ceramidase inhibitors induces a significant increase in ABCA12 mRNA levels (Fig. 6*E*). Together, these results indicate that inhibition of ceramidase activity increases endogenous ceramide levels, leading to a stimulation of ABCA12 expression. Additionally, the metabolism of C_6-Cer via the ceramidase pathway is not required for C_6-Cer-induced ABCA12 gene expression.

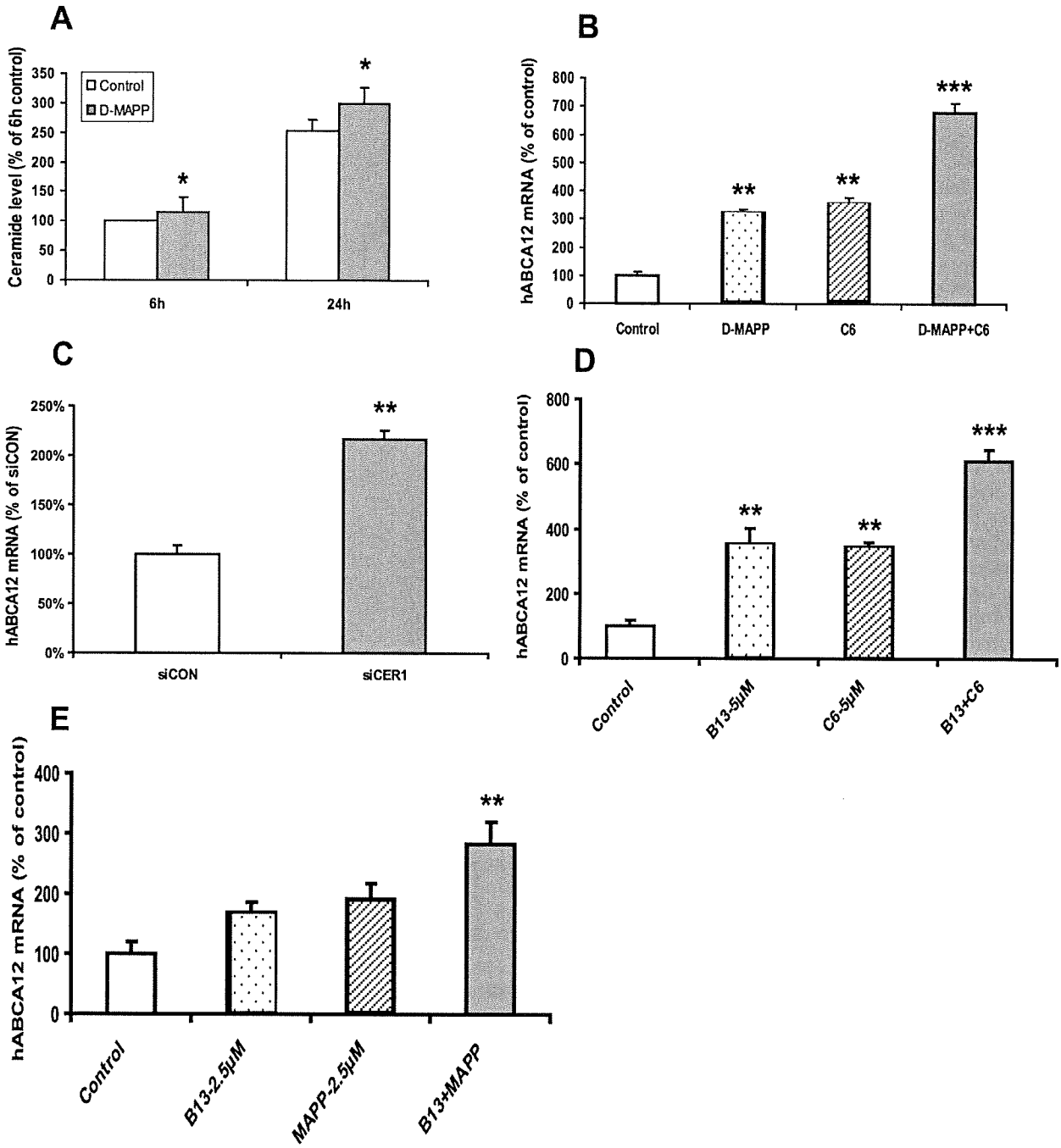

FIGURE 6. **Ceramidase inhibitors increase endogenous ceramide levels and induce ABCA12 mRNA.** *A*, cultured human keratinocytes were incubated with vehicle (*open bars*) or D-MAPP (10 μM; *solid bars*) for 6 or 24 h, and ceramide levels were determined ($n = 4$). *B*, cells were incubated with vehicle, D-MAPP (10 μM; *dotted bar*), C_6-Cer (5 μM; *hatched bar*), or D-MAPP plus C_6-Cer for 16 h ($n = 3$). *C*, cells were transiently transfected with specific alkaline ceramidase-1 siRNA (*solid bar*) or control siRNA (*open bar*) ($n = 4$). *D*, cells were incubated with vehicle control, B13 (5 μM), C_6-Cer (5 μM), or B13 plus C_6-Cer for 16 h ($n = 3$). *E*, cells were incubated with vehicle, B13 (2.5 μM), D-MAPP (2.5 μM), or B13 plus D-MAPP for 16 h. ABCA12 mRNA levels were measured in cells (*B–E*), and data are expressed as a percentage of control (100%) and presented as mean ± S.E. Experiment was repeated at least once with similar results. *, $p < 0.05$; **, $p < 0.01$; ***, $p < 0.001$; C6: C_6-Cer.

Ceramides are well known to cause toxicity and apoptosis in some cell lines. Hence, during the course of our experiments, both trypan blue staining, a marker of cell toxicity, and a TUNEL assay, a marker of apoptosis, were performed. After 16 h of incubation, we observed that trypan blue staining was 82% in controls *versus* 84% in the C_6-Cer (5 μM)-treated cells ($n = 3$; repeated once with similar results), indicating that C_6-Cer did not cause cell toxicity. Similarly, following a 20-h incubation of cells with vehicle, C_6-Cer (5 μM), D-PPMP (5 μM), D-MAPP (15 μM), or C_6-Cer plus D-PPMP/D-MAPP, the apoptotic cell number was less than 3% in all groups ($n = 3$; repeated once with similar results), indicating that these treatments do not induce apoptosis

in keratinocytes under these culture conditions. Thus, under our experimental condition, the cells are healthy and do not exhibit any increased toxicity or apoptosis.

Blocking de Novo Synthesis of Ceramide Does Not Affect ABCA12 mRNA Expression—Previous studies have shown that *de novo* ceramide synthesis is robust in epidermis/keratinocytes (32, 38). Since exogenously added ceramide induces ABCA12 expression, we next examined whether blocking ceramide biosynthesis would decrease ABCA12 expression. Myriosin and βCA are inhibitors of serine-palmitoyl transferase, the key enzyme for initiating *de novo* biosynthesis of ceramides (39, 40) (Fig. 1). However, treatment with either myriocin or βCA failed to alter ABCA12 expression (data not shown). Furthermore, fumonisin B1, a mycotoxin that inhibits the activity of another key enzyme required for ceramide synthesis (Fig. 1), ceramide synthase (sphingosine *N*-acyltransferase) (41, 42), also did not alter ABCA12 expression (data not shown). Previously, we reported that treatment with either βCA or fumonisin B1 decreases intracellular ceramide levels in cultured human keratinocytes (40). Thus, inhibiting *de novo* ceramide biosynthesis of ceramide did not affect ABCA12 expression.

Ceramide Induces ABCA12 Gene Expression via the PPARδ Signaling Pathway—Previously, we reported that activation of PPARδ markedly stimulates ABCA12 expression in cultured human keratinocytes (18). Furthermore, activation of PPARδ also stimulates both ceramide and lamellar body formation (20). To investigate whether ceramide increases ABCA12 gene expression via the PPARδ pathway, we initially examined the effect of ceramide treatment on expression levels of PPAR (α, δ, and γ), or LXR (α and β). C_6-Cer preferentially increased PPARδ mRNA levels (~4 fold) (Fig. 7*A*). In contrast, C_6-Cer had limited effects on PPARα, PPARγ, LXR-α, or LXR-β mRNA levels (Fig. 7*A*). Similar results were obtained when keratinocytes were incubated with C_2-Cer (data not shown). C_6-Cer also elevated PPARδ mRNA levels dose-dependently (Fig. 7*B*), and similar results were obtained for C_2-Cer treatment (data not shown). Accordingly, C_6-Cer markedly enhanced PPARδ protein levels (Fig. 7*C*).

In parallel to what was seen with ABCA12, inhibitors of glucosyltransferase, such as D-PMPP and P4, increased PPARδ mRNA levels (Fig. 8, *A* and *B*). Furthermore, both D-PMPP (Fig. 8*A*) and P4 (Fig. 8*B*) were additive with C_6-Cer in inducing PPARδ mRNA. Similarly, other inhibitors, such as D-MAPP, also increased PPARδ mRNA levels and were additive to C_6-Cer (Fig. 8*C*). Thus, both exogenous and endogenous ceramides up-regulate PPARδ mRNA expression.

Finally, to determine if this increase in PPARδ expression could mediate the C_6-Cer-induced increase in ABCA12 expression, we examined whether PPARδ knockdown by siRNA transfection would attenuate the increase in ABCA12 expression by exogenous ceramide. The siRNA knocked down PPARδ mRNA levels by ~70% (Fig. 9*A*). In parallel, the PPARδ siRNA transfection greatly diminished the C_6-Cer-induced increase in PPARδ mRNA levels (Fig. 9*A*). Accordingly, although C_6-Cer significantly increased ABCA12 mRNA levels in keratinocytes transfected with negative control siRNA, this increase was markedly attenuated (~70%) by PPARδ siRNA transfection (Fig. 9*B*). In contrast, the C_6-Cer-induced increase in mRNA levels of involucrin, a differentiation marker of keratinocytes, was not significantly attenuated by PPARδ siRNA transfection (Fig. 9*C*). Together, these results indicate that the C_6-Cer-induced increase in ABCA12 mRNA levels is mediated at least in part by PPARδ, since C_6-Cer preferentially stimulated PPARδ expression, and knocking down PPARδ by siRNA transfection specifically attenuated the mRNA levels of ABCA12 but not other C_6-Cer-inducible mRNA levels (involucrin).

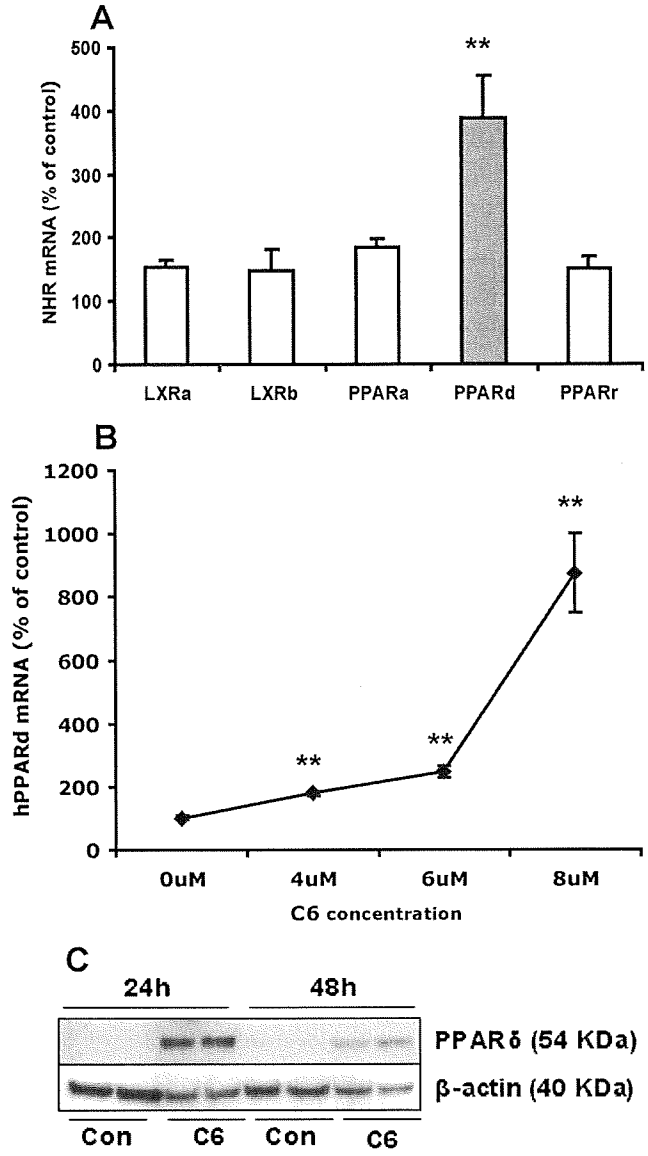

FIGURE 7. **Exogenous C_6-Cer preferentially stimulates PPARδ expression.** Cultured human keratinocytes were incubated with C_6-Cer (5 μM) or vehicle for 16 h, and mRNA levels of PPARα, PPARδ, PPARγ, LXR-α, and LXR-β were measured (*A*). Alternatively, cells were treated with vehicle or various doses (0, 4, 6, and 8 μM) of C_6-Cer for 24 h (*B*), and PPARδ mRNA levels were measured, expressed as a percentage of control (100%) and presented as mean ± S.E. ($n = 4$). In an another set of cells, following C_6-Cer (5 μM) or vehicle treatment for 24 or 48 h, PPARδ protein levels (*C*) were measured as described under "Experimental Procedures." Experiments were repeated at least once with similar results. *, $p < 0.05$; **, $p < 0.01$. *Con*, control; C6: C_6-Cer.

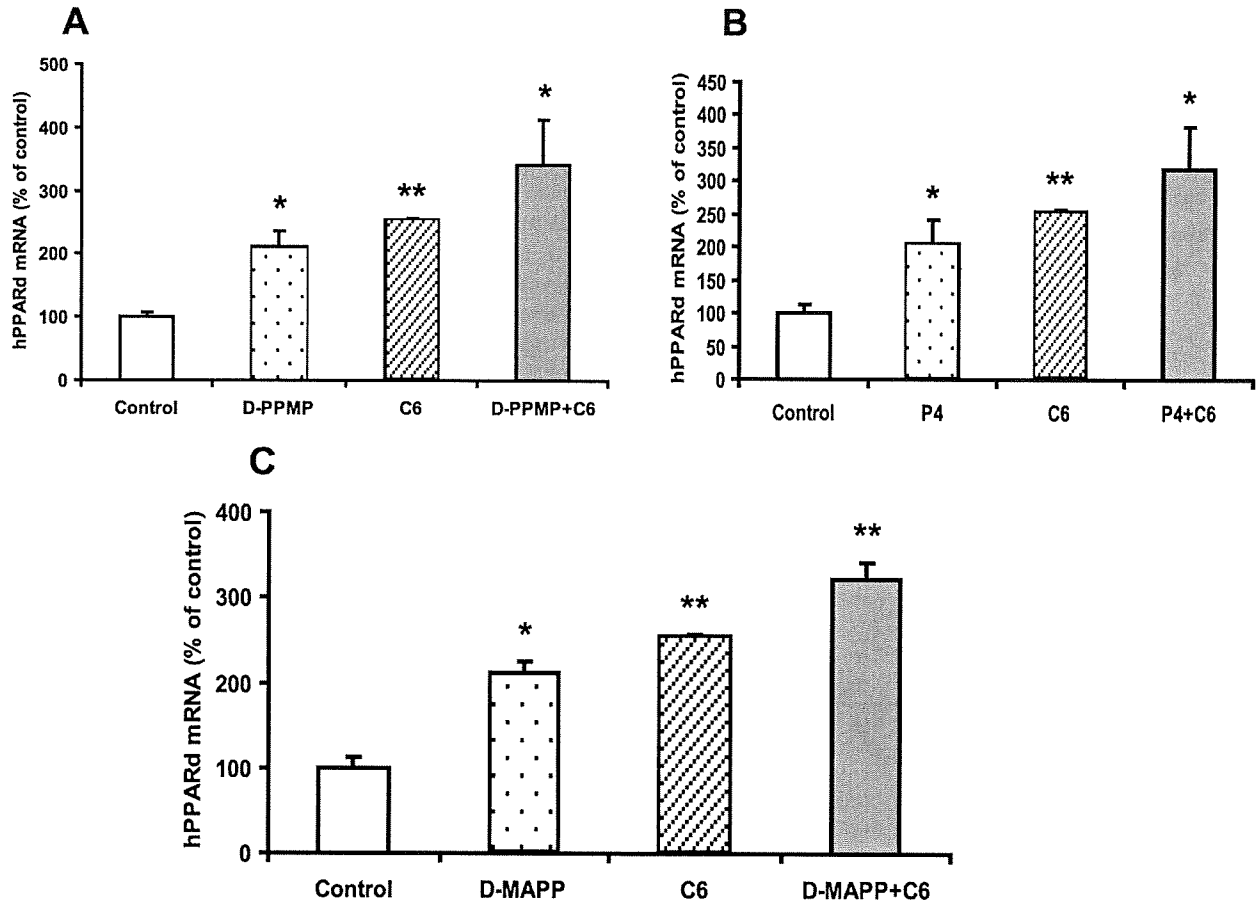

FIGURE 8. **Increasing endogenous ceramides by inhibiting glucosylceramide synthase or ceramidase stimulate PPARδ expression.** Cultured human keratinocytes were incubated with vehicle, D-PPMP (5 μM), C_6-Cer (5 μM), or D-PPMP plus C_6-Cer for 16 h (*A*). Alternatively, cells were incubated with vehicle, P4 (10 μM), C_6-Cer (5 μM), or P4 plus C_6-Cer in the same medium for 16 h (*B*). In another set of experiments, cells were incubated with vehicle, D-MAPP (10 μM), C_6-Cer (5 μM), or D-MAPP plus C_6-Cer in the same medium for 16 h (*C*). PPARδ mRNA levels were measured, expressed as a percentage of control (100%), and presented as mean ± S.E. ($n = 3$). Experiments were repeated at least once with similar results. *, $p < 0.05$; **, $p < 0.01$; C: C_6-Cer.

DISCUSSION

ABCA12 plays an essential role in permeability barrier formation, since human mutations and knock-out mice have defective barriers, due to abnormal lamellar body formation (5, 14, 43). In this study, we demonstrate that ceramides, the precursor of glucosylceramides (Fig. 1), stimulate ABCA12 expression by a PPARδ-dependent mechanism.

First, we showed that exogenous, synthetic, cell-permeable ceramides, C_6-Cer and C_2-Cer, when incubated with human keratinocytes, increase the mRNA and protein levels of ABCA12. In contrast, sphingosine, sphinganine, glucosylceramide, or ceramide 1-phosphate did not alter *ABCA12* gene expression. Second, increasing endogenous ceramide levels also stimulated ABCA12 expression. Blocking the conversion of ceramide to glucosylceramide by glucosylceramide synthase inhibitors, inhibiting sphingomyelin synthesis from ceramides by sphingomyelin synthase inhibitors, and blocking the hydrolysis of ceramides to sphingosine by ceramidase inhibitors all increased cellular ceramide levels and concomitantly increased ABCA12 mRNA levels. Thus, both short-chain, exogenous added synthetic ceramides and long-chain, endogenously produced ceramides stimulate *ABCA12* gene expression. However, blocking *de novo* ceramide synthesis with a number of different inhibitors did not decrease ABCA12 expression. This may simply indicate that the basal expression of ABCA12 is regulated by other factors and is not dependent on ceramide levels. Alternatively, it is possible that inhibiting *de novo* ceramide synthesis diminishes a cellular pool that does not regulate ABCA12 expression.

Our studies further suggest that ceramides *per se* and not metabolites derived from ceramides (see Fig. 1) regulate ABCA12 gene expression. Blocking the conversion of ceramides into glucosylceramides or sphingomyelin by inhibitors did not decrease the ability of C_6-Cer to increase ABCA12 mRNA levels. Similarly, blocking ceramidase activity, which is required for the formation of sphingosine and sphingosine 1-phosphate, also did not decrease the ability of C_6-Cer to increase ABCA12 mRNA levels. Additionally, as noted above, sphingosine, sphinganine, ceramide 1-phosphate, and glucosylceramide did not alter *ABCA12* gene expression. Together, these results suggest that ceramides directly regulate ABCA12 expression. However, since the specific molecular pathway by which ceramides increase ABCA12 expression has not been fully elucidated, one can-

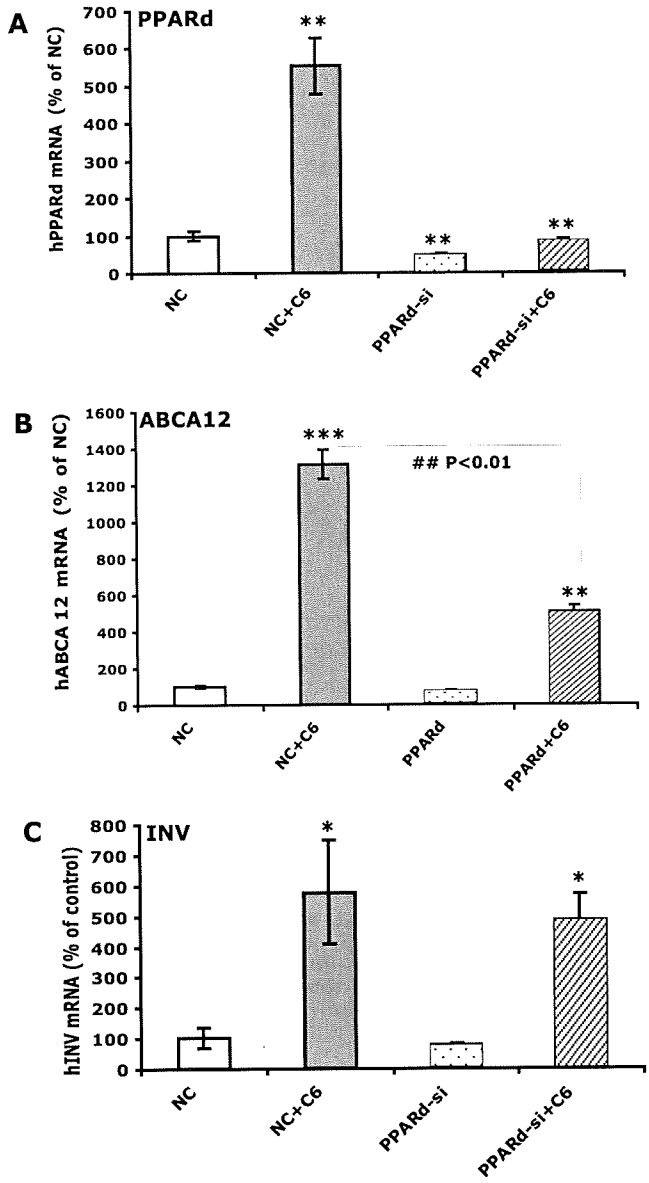

FIGURE 9. **Decreasing PPARδ by siRNA specifically attenuates C_6-Cer-induced *ABCA12* gene expression.** Cultured human keratinocytes were transiently transfected with a specific human PPARδ siRNA or negative control siRNA, followed by treatment with either vehicle or C_6-Cer (5 μM) for 24 h. Messenger RNA levels of PPARδ (*A*), ABCA12 (*B*), and involucrin (*C*) were measured ($n = 4$) as described under "Experimental Procedures." Data are expressed as a percentage of negative control (100%) and presented as mean ± S.E. Experiments were repeated twice with similar results. **, $p < 0.01$; ***, $p < 0.001$ (*versus* negative control). ##, $p < 0.01$ (*versus* vehicle). *NC*, negative control; *PPARd-si*, PPARδ siRNA; *INV*, involucrin; C6: C_6-Cer.

not rule out the formation of an alternative ceramide metabolite accounting for the effect.

The involvement of ceramides in gene regulation has been well documented. In cultured keratinocytes, synthetic C_6-Cer and C_2-Cer have been shown to inhibit cell proliferation and to promote cell differentiation (44). In addition, ceramide enhances glucosylceramide synthase activity via increasing gene transcription (45, 46) and induces acid sphingomyelinase expression (47, 48). Ceramides have also been shown to directly stimulate the transcription of cyclooxygenase-2 in human breast epithelial cells (49) and indirectly mediate the tumor necrosis factor α-induced increase in cyclooxygenase-2 expression in human alveolar epithelial cells (50). In this study, we demonstrated that ceramides stimulate the expression of ABCA12, an important transporter for glucosylceramides. One can view this as a feed-forward effect. As the keratinocyte begins to produce increasing quantities of ceramides that will lead to increased glucosylceramide synthesis, the ceramides signal the cell to increase ABCA12 levels, which will facilitate the transport of glucosylceramides into lamellar bodies. To further support this notion, Zuo *et al.* (16) recently revealed that loss of ABCA12 transport function by generating *Abca12*$^{-/-}$ mice causes a 90% reduction in epidermal linoleic esters of long-chain ω-hydroxy-ceramides, associated with an increase in their glucosyl ceramide precursors. Thus, the ceramides serve not only as a precursor of glucosylceramide formation but also as a signaling molecule that will allow the keratinocyte to transport the glucosylceramide to the appropriate location within the lamellar body.

To further elucidate the mechanism underlying the ceramide-induced stimulation of ABCA12 expression, we carried out time course studies and noted that the increase in ABCA12 mRNA occurs only after a ~9-h incubation, suggesting a secondary rather than a direct stimulatory effect. Previous studies by our laboratory (18) have shown that activation of PPARδ stimulates ABCA12 expression. These observations prompted us to hypothesize that ceramide might induce ABCA12 expression via PPARδ. Our results demonstrate that PPARδ signaling does play an important role in the ceramide-induced stimulation of ABCA12 expression in keratinocytes. First, C_6-Cer increases PPARδ expression at both mRNA and protein levels. Second, the stimulatory effect on PPARδ expression is not limited to exogenous ceramides but also was seen with increases in endogenously produced ceramides. In contrast, ceramides did not increase the expression of PPARα, PPARγ, LXR-α, or LXR-β. Third, PPARδ mRNA silencing by siRNA transfection results in a significant attenuation of the ceramide-induced increase in *ABCA12* gene expression. This attenuation effect of ceramides on ABCA12 is specific, since the ability of ceramides to induce other genes, such as involucrin, was not altered by decreasing PPARδ.

Thus, the ceramide-induced stimulation of ABCA12 gene expression is an indirect effect and probably involves multiple steps. Studies have shown that the expression of PPARδ is increased by AP-1 activation (51). Moreover, numerous studies have shown that ceramides increase AP-1 activity in keratinocytes and other cells (51–55). We would therefore hypothesize that ceramides increase AP-1 activity, leading to the increased expression of PPARδ, which subsequently stimulates ABCA12 gene expression.

PPARδ is the most abundant PPAR isoform in keratinocytes and is found throughout all layers of the epidermis (56). In human keratinocytes, PPARδ plays an important role in regulating gene expression and regulates epidermal proliferation, differentiation, and wound healing (19, 57). For example, activation of PPARδ stimulates the expression of proteins, including involucrin, loricrin, filaggrin, and transglutaminase 1, required for the differentiation of keratinocytes into corneo-

cytes (58, 59). PPARδ activation also improves epidermal permeability barrier homeostasis by stimulating epidermal lipid biosynthesis, including *de novo* ceramide synthesis (20). Finally, activation of PPARδ increases β-glucocerebrosidase activity in the stratum corneum (20), a key enzyme required for the conversion of glucosylceramides to ceramides and the formation of normal lamellar membranes. Whether the ability of ceramides to increase PPARδ expression will account for most of the observed effects of ceramides on keratinocytes remains to be determined. However, it should be noted that the increase in involucrin expression induced by ceramide is not mediated by PPARδ signaling. Nonetheless, our study demonstrated that PPARδ mediates the ceramide-induced ABCA12 expression in keratinocytes.

In summary, our results show that ceramide, an important lipid component of epidermis, up-regulates ABCA12 expression via the PPARδ signaling pathway, providing a substrate-driven, feed-forward mechanism for regulating this key lipid transporter required for lamellar body formation.

Acknowledgment—We thank Sally Pennypacker for the excellent technical support of cell culture.

REFERENCES

1. Feingold, K. R. (2007) *J. Lipid Res.* **48,** 2531–2546
2. Elias, P. M., and Feingold, K. R. (ed) (2006) *Epidermal Lamellar Body as A Multifunctional Secretory Organelle*, pp. 261–272, Taylor & Francis, New York
3. Grayson, S., Johnson-Winegar, A. G., Wintroub, B. U., Isseroff, R. R., Epstein, E. H., Jr., and Elias, P. M. (1985) *J. Invest. Dermatol.* **85,** 289–294
4. Holleran, W. M., Takagi, Y., and Uchida, Y. (2006) *FEBS Lett.* **580,** 5456–5466
5. Akiyama, M., Sugiyama-Nakagiri, Y., Sakai, K., McMillan, J. R., Goto, M., Arita, K., Tsuji-Abe, Y., Tabata, N., Matsuoka, K., Sasaki, R., Sawamura, D., and Shimizu, H. (2005) *J. Clin. Invest.* **115,** 1777–1784
6. Hovnanian, A. (2005) *J. Clin. Invest.* **115,** 1708–1710
7. Akiyama, M. (2006) *Arch. Dermatol.* **142,** 914–918
8. Bodzioch, M., Orsó, E., Klucken, J., Langmann, T., Böttcher, A., Diederich, W., Drobnik, W., Barlage, S., Büchler, C., Porsch-Ozcürümez, M., Kaminski, W. E., Hahmann, H. W., Oette, K., Rothe, G., Aslanidis, C., Lackner, K. J., and Schmitz, G. (1999) *Nat. Genet.* **22,** 347–351
9. Brooks-Wilson, A., Marcil, M., Clee, S. M., Zhang, L. H., Roomp, K., van Dam, M., Yu, L., Brewer, C., Collins, J. A., Molhuizen, H. O., Loubser, O., Ouelette, B. F., Fichter, K., Ashbourne-Excoffon, K. J., Sensen, C. W., Scherer, S., Mott, S., Denis, M., Martindale, D., Frohlich, J., Morgan, K., Koop, B., Pimstone, S., Kastelein, J. J., Genest, J., Jr., and Hayden, M. R. (1999) *Nat. Genet.* **22,** 336–345
10. Lawn, R. M., Wade, D. P., Garvin, M. R., Wang, X., Schwartz, K., Porter, J. G., Seilhamer, J. J., Vaughan, A. M., and Oram, J. F. (1999) *J. Clin. Invest.* **104,** R25–31
11. Rust, S., Rosier, M., Funke, H., Real, J., Amoura, Z., Piette, J. C., Deleuze, J. F., Brewer, H. B., Duverger, N., Denèfle, P., and Assmann, G. (1999) *Nat. Genet.* **22,** 352–355
12. Shulenin, S., Nogee, L. M., Annilo, T., Wert, S. E., Whitsett, J. A., and Dean, M. (2004) *N. Engl. J. Med.* **350,** 1296–1303
13. Allikmets, R. (1997) *Nat. Genet.* **17,** 122
14. Lefévre, C., Audebert, S., Jobard, F., Bouadjar, B., Lakhdar, H., Boughdene-Stambouli, O., Blanchet-Bardon, C., Heilig, R., Foglio, M., Weissenbach, J., Lathrop, M., Prud'homme, J. F., and Fischer, J. (2003) *Hum. Mol. Genet.* **12,** 2369–2378
15. Kelsell, D. P., Norgett, E. E., Unsworth, H., Teh, M. T., Cullup, T., Mein, C. A., Dopping-Hepenstal, P. J., Dale, B. A., Tadini, G., Fleckman, P., Stephens, K. G., Sybert, V. P., Mallory, S. B., North, B. V., Witt, D. R., Spreecher, E., Taylor, A. E., Ilchyshyn, A., Kennedy, C. T., Goodyear, H., Moss, C., Paige, D., Harper, J. I., Young, B. D., Leigh, I. M., Eady, R. A., and O'Toole, E. A. (2005) *Am. J. Hum. Genet.* **76,** 794–803
16. Zuo, Y., Zhuang, D. Z., Han, R., Isaac, G., Tobin, J. J., McKee, M., Welti, R., Brissette, J. L., Fitzgerald, M. L., and Freeman, M. W. (2008) *J. Biol. Chem.* **283,** 36624–36635
17. Moskowitz, D. G., Fowler, A. J., Heyman, M. B., Cohen, S. P., Crumrine, D., Elias, P. M., and Williams, M. L. (2004) *J. Pediatr.* **145,** 82–92
18. Jiang, Y. J., Lu, B., Kim, P., Paragh, G., Schmitz, G., Elias, P. M., and Feingold, K. R. (2008) *J. Invest. Dermatol.* **128,** 104–109
19. Schmuth, M., Jiang, Y. J., Dubrac, S., Elias, P. M., and Feingold, K. R. (2008) *J. Lipid Res.* **49,** 499–509
20. Man, M. Q., Choi, E. H., Schmuth, M., Crumrine, D., Uchida, Y., Elias, P. M., Holleran, W. M., and Feingold, K. R. (2006) *J. Invest. Dermatol.* **126,** 386–392
21. Chang, K. C., Shen, Q., Oh, I. G., Jelinsky, S. A., Jenkins, S., Wang, W., Wang, Y., Lacava, M., Yudt, M. R., Thompson, C. C., Freedman, L. P., Chung, J. H., and Nagpal, S. (2008) *Mol. Endocrinol.* **22,** 2407–2419
22. Lampe, M. A., Williams, M. L., and Elias, P. M. (1983) *J. Lipid Res.* **24,** 131–140
23. Vielhaber, G., Pfeiffer, S., Brade, L., Lindner, B., Goldmann, T., Vollmer, E., Hintze, U., Wittern, K. P., and Wepf, R. (2001) *J. Invest. Dermatol.* **117,** 1126–1136
24. Geilen, C. C., Bektas, M., Wieder, T., Kodelja, V., Goerdt, S., and Orfanos, C. E. (1997) *J. Biol. Chem.* **272,** 8997–9001
25. Hannun, Y. A., and Obeid, L. M. (2002) *J. Biol. Chem.* **277,** 25847–25850
26. Uchida, Y., Nardo, A. D., Collins, V., Elias, P. M., and Holleran, W. M. (2003) *J. Invest. Dermatol.* **120,** 662–669
27. Spiegel, S., and Milstien, S. (2002) *J. Biol. Chem.* **277,** 25851–25854
28. Jiang, Y. J., Lu, B., Kim, P., Elias, P. M., and Feingold, K. R. (2006) *J. Lipid Res.* **47,** 2248–2258
29. Venkateswaran, A., Laffitte, B. A., Joseph, S. B., Mak, P. A., Wilpitz, D. C., Edwards, P. A., and Tontonoz, P. (2000) *Proc. Natl. Acad. Sci. U.S.A.* **97,** 12097–12102
30. Akiyama, M., Titeux, M., Sakai, K., McMillan, J. R., Tonasso, L., Calvas, P., Jossic, F., Hovnanian, A., and Shimizu, H. (2007) *J. Invest. Dermatol.* **127,** 568–573
31. Neish, A. S., Khachigian, L. M., Park, A., Baichwal, V. R., and Collins, T. (1995) *J. Biol. Chem.* **270,** 28903–28909
32. Holleran, W. M., Man, M. Q., Gao, W. N., Menon, G. K., Elias, P. M., and Feingold, K. R. (1991) *J. Clin. Invest.* **88,** 1338–1345
33. Bligh, E. G., and Dyer, W. J. (1959) *Can. J. Biochem. Physiol.* **37,** 911–917
34. Houben, E., Holleran, W. M., Yaginuma, T., Mao, C., Obeid, L. M., Rogiers, V., Takagi, Y., Elias, P. M., and Uchida, Y. (2006) *J. Lipid Res.* **47,** 1063–1070
35. Bielawska, A., Greenberg, M. S., Perry, D., Jayadev, S., Shayman, J. A., McKay, C., and Hannun, Y. A. (1996) *J. Biol. Chem.* **271,** 12646–12654
36. Selzner, M., Bielawska, A., Morse, M. A., Rudiger, H. A., Sindram, D., Hannun, Y. A., and Clavien, P. A. (2001) *Cancer Res.* **61,** 1233–1240
37. Fishelevich, R., Malanina, A., Luzina, I., Atamas, S., Smyth, M. J., Porcelli, S. A., and Gaspari, A. A. (2006) *J. Immunol.* **176,** 2590–2599
38. Holleran, W. M., Williams, M. L., Gao, W. N., and Elias, P. M. (1990) *J. Lipid Res.* **31,** 1655–1661
39. Miyake, Y., Kozutsumi, Y., Nakamura, S., Fujita, T., and Kawasaki, T. (1995) *Biochem. Biophys. Res. Commun.* **211,** 396–403
40. Uchida, Y., Murata, S., Schmuth, M., Behne, M. J., Lee, J. D., Ichikawa, S., Elias, P. M., Hirabayashi, Y., and Holleran, W. M. (2002) *J. Lipid Res.* **43,** 1293–1302
41. Merrill, A. H., Jr., van Echten, G., Wang, E., and Sandhoff, K. (1993) *J. Biol. Chem.* **268,** 27299–27306
42. Merrill, A. H., Jr., Sullards, M. C., Wang, E., Voss, K. A., and Riley, R. T. (2001) *Environ. Health Perspect.* **109,** Suppl. 2, 283–289
43. Yanagi, T., Akiyama, M., Nishihara, H., Sakai, K., Nishie, W., Tanaka, S., and Shimizu, H. (2008) *Hum. Mol. Genet.* **17,** 3075–3083
44. Wakita, H., Tokura, Y., Yagi, H., Nishimura, K., Furukawa, F., and Takigawa, M. (1994) *Arch. Dermatol. Res.* **286,** 350–354
45. Liu, Y. Y., Yu, J. Y., Yin, D., Patwardhan, G. A., Gupta, V., Hirabayashi, Y., Holleran, W. M., Giuliano, A. E., Jazwinski, S. M., Gouaze-Andersson, V.,

Consoli, D. P., and Cabot, M. C. (2008) *FASEB J.* **22,** 2541–2551
46. Komori, H., Ichikawa, S., Hirabayashi, Y., and Ito, M. (2000) *FEBS Lett.* **475,** 247–250
47. Deigner, H. P., Claus, R., Bonaterra, G. A., Gehrke, C., Bibak, N., Blaess, M., Cantz, M., Metz, J., and Kinscherf, R. (2001) *FASEB J.* **15,** 807–814
48. Murate, T., Suzuki, M., Hattori, M., Takagi, A., Kojima, T., Tanizawa, T., Asano, H., Hotta, T., Saito, H., Yoshida, S., and Tamiya-Koizumi, K. (2002) *J. Biol. Chem.* **277,** 9936–9943
49. Subbaramaiah, K., Chung, W. J., and Dannenberg, A. J. (1998) *J. Biol. Chem.* **273,** 32943–32949
50. Chen, C. C., Sun, Y. T., Chen, J. J., and Chang, Y. J. (2001) *Mol. Pharmacol.* **59,** 493–500
51. Tan, N. S., Michalik, L., Noy, N., Yasmin, R., Pacot, C., Heim, M., Flühmann, B., Desvergne, B., and Wahli, W. (2001) *Genes Dev.* **15,** 3263–3277
52. Westwick, J. K., Bielawska, A.-E., Dbaibo, G., Hannun, Y. A., and Brenner, D. A. (1995) *J. Biol. Chem.* **270,** 22689–22692
53. Zhao, Y., Nichols, J. E., Valdez, R., Mendelson, C. R., and Simpson, E. R. (1996) *Mol. Endocrinol.* **10,** 1350–1357
54. Quillet-Mary, A., Jaffrézou, J. P., Mansat, V., Bordier, C., Naval, J., and Laurent, G. (1997) *J. Biol. Chem.* **272,** 21388–21395
55. Reunanen, N., Westermarck, J., Häkkinen, L., Holmström, T. H., Elo, I., Eriksson, J. E., and Kähäri, V. M. (1998) *J. Biol. Chem.* **273,** 5137–5145
56. Braissant, O., and Wahli, W. (1998) *Endocrinology* **139,** 2748–2754
57. Schmuth, M., Jiang, Y. J., Dubrac, S., Elias, P. M., and Feingold, K. R. (2008) *J. Lipid Res.* **49,** 499–509
58. Westergaard, M., Henningsen, J., Svendsen, M. L., Johansen, C., Jensen, U. B., Schrøder, H. D., Kratchmarova, I., Berge, R. K., Iversen, L., Bolund, L., Kragballe, K., and Kristiansen, K. (2001) *J. Invest. Dermatol.* **116,** 702–712
59. Schmuth, M., Haqq, C. M., Cairns, W. J., Holder, J. C., Dorsam, S., Chang, S., Lau, P., Fowler, A. J., Chuang, G., Moser, A. H., Brown, B. E., Mao-Qiang, M., Uchida, Y., Schoonjans, K., Auwerx, J., Chambon, P., Willson, T. M., Elias, P. M., and Feingold, K. R. (2004) *J. Invest. Dermatol.* **122,** 971–983

The American Journal of Pathology, Vol. 175, No. 6, December 2009

DOI: 10.2353/ajpath.2009.090347

Molecular Pathogenesis of Genetic and Inherited Diseases

Keratinocyte-/Fibroblast-Targeted Rescue of *Col7a1*-Disrupted Mice and Generation of an Exact Dystrophic Epidermolysis Bullosa Model Using a Human *COL7A1* Mutation

Kei Ito,* Daisuke Sawamura,* Maki Goto,* Hideki Nakamura,* Wataru Nishie,* Kaori Sakai,* Ken Natsuga,* Satoru Shinkuma,* Akihiko Shibaki,* Jouni Uitto,† Christopher P. Denton,‡ Osamu Nakajima,§ Masashi Akiyama,* and Hiroshi Shimizu*

From the Department of Dermatology, Hokkaido University Graduate School of Medicine, Sapporo, Japan; Department of Dermatology and Cutaneous Biology,† Jefferson Medical College and Jefferson Institute of Molecular Medicine, Thomas Jefferson University, Philadelphia, Pennsylvania; Department of Medicine,‡ Royal Free Campus, University College London, London, United Kingdom; and Research Laboratory for Molecular Genetics,§ Yamagata University, Yamagata, Japan*

Recessive dystrophic epidermolysis bullosa (RDEB) is a severe hereditary bullous disease caused by mutations in *COL7A1*, which encodes type VII collagen (COL7). *Col7a1* knockout mice ($COL7^{m-/-}$) exhibit a severe RDEB phenotype and die within a few days after birth. Toward developing novel approaches for treating patients with RDEB, we attempted to rescue $COL7^{m-/-}$ mice by introducing human *COL7A1* cDNA. We first generated transgenic mice that express human *COL7A1* cDNA specifically in either epidermal keratinocytes or dermal fibroblasts. We then performed transgenic rescue experiments by crossing these transgenic mice with $COL7^{m+/-}$ heterozygous mice. Surprisingly, human COL7 expressed by keratinocytes or by fibroblasts was able to rescue all of the abnormal phenotypic manifestations of the $COL7^{m-/-}$ mice, indicating that fibroblasts as well as keratinocytes are potential targets for RDEB gene therapy. Furthermore, we generated transgenic mice with a premature termination codon expressing truncated COL7 protein and performed the same rescue experiments. Notably, the $COL7^{m-/-}$ mice rescued with the human *COL7A1* allele were able to survive despite demonstrating clinical manifestations very similar to those of human RDEB, indicating that we were able to generate surviving animal models of RDEB with a mutated human *COL7A1* gene. This model has great potential for future research into the pathomechanisms of dystrophic epidermolysis bullosa and the development of gene therapies for patients with dystrophic epidermolysis bullosa. ***(Am J Pathol 2009, 175:000–000; DOI: 10.2353/ajpath.2009.090347)***

Dystrophic epidermolysis bullosa (DEB) is clinically characterized by mucocutaneous blistering in response to minor trauma, followed by scarring and nail dystrophy. The blistering occurs along the epidermal basement membrane zone (BMZ) just beneath the lamina densa at the level of the anchoring fibrils. The inheritance of DEB can be autosomal dominant (DDEB) or autosomal recessive (RDEB), each comprising subtypes of different clinical presentations and severities.[1] Both DDEB and RDEB are known to be caused by mutations in the *COL7A1* gene encoding type VII collagen (COL7), the major component of anchoring fibrils.[2] The most severe RDEB subtype, the Hallopeau-Siemens subtype, shows a complete lack of expression of type VII collagen, whereas a less severe RDEB subtype, the non-Hallopeau-Siemens subtype, shows some collagen expression. The clinical fea-

Supported in part by a Grant-in-Aid for Scientific Research from the Japanese Society for the Promotion of Science, by a grant from Ministry of Health, Labour and Welfare of Japan (Health and Labour Sciences Research Grants; Research on Intractable Diseases) and by the National Institute of Arthritis & Musculoskeletal & Skin Diseases, National Institutes of Health (grant R01-AR54876-01).

K.I. and D.S. contributed equally to this work.

Accepted for publication August 20, 2009.

A guest editor acted as editor-in-chief for this manuscript. No person at Thomas Jefferson University was involved in the peer review process or final disposition for this article.

Address reprint requests to Hiroshi Shimizu M.D., Ph.D., Department of Dermatology, Hokkaido University Graduate School of Medicine, N15 W7, Kita-ku, Sapporo 060-8638, Japan. E-mail: shimizu@med.hokudai.ac.jp

tures of DDEB are, in general, milder than those of RDEB and tend to improve with age. The molecular mechanisms of DEB have been thoroughly investigated, and precise diagnosis and estimation of prognosis is now possible. There is no specific treatment for different forms of DEB, and the current focus of research is to develop more effective treatments for this group of blistering disorders.

Corrective gene therapy whereby normal COL7 is introduced into the patients' cells, has great potential as a treatment for DEB. However, several obstacles must be overcome before its clinical therapeutic application. First, there have been no useful DEB animal models that reproduce the human mutated gene for experiments. Although COL7 knockout mice have been generated, most of such mice die within a few days of birth, and none survive more than 2 weeks.[3] A surviving DEB mouse that was reported recently was the DEB hypomorphic mouse model.[4] These mice, which had about 10% of the normal mouse COL7, did not show the abnormal form and function of anchoring fibrils seen in human patients of RDEB. Second, no studies have examined in detail whether the introduction of the human COL7 gene into DEB mouse cells can rescue the DEB phenotype without causing adverse effects in a living DEB model. Third, there is controversy over which cells may serve as optimal targets in gene therapies for DEB. Several studies have targeted keratinocytes, because the cells that secrete COL7 are mainly keratinocytes and to a lesser extent fibroblasts.[5,6] However, we and others have recently reported that injection of gene-transferred fibroblasts into the skin can efficiently restore COL7 expression in the dermal-epidermal junction *in vitro*.[6–8] Furthermore, intradermal injection of allogeneic fibroblasts into skin of patients with RDEB skin was shown to result in enhanced COL7 expression in selected patients.[9] Therefore, we need to compare keratinocytes and fibroblasts to clarify their efficacy as target cells in an *in vivo* model system of RDEB.

To address these issues, we generated transgenic mice with human *COL7A1* under different promoters and performed transgenic rescue experiments on the Col7a1$^{m-/-}$ background using those transgenic mice. Furthermore, to develop a DEB model that accurately reproduces human DEB not only in terms of clinical manifestations but also in terms of gene mutation, we also introduced a mutated human *COL7A1* gene into this mouse model system and created human mutant gene-expressing rescued mice corresponding to the surviving animal of DEB. Our results advance our understanding of the function and biology of COL7.

Materials and Methods

Generation of Transgenic Mice

Human full-length *COL7A1* cDNA was constructed from several overlapping cDNA clones (Sawamura et al, 2002). We used a pCMVβ expression vector (Invitrogen, Carlsbad, CA) that contained the cytomegalovirus (CMV) promoter, the simian virus 40 (SV40) splice donor/splice acceptor site, the *lacZ* gene, and the SV40 polyadenylation signal. We selected human keratin 14 (K14),[10] the mouse pro-α 2 chain of type I collagen (col1a2),[11] or the CMV promoter for epidermis-specific, dermis-specific, or ubiquitous expression of the transgene, respectively. We first modified pCMVβ by replacing LacZ with human full-length *COL7A1* cDNA, and the CMV promoter with the human K14 or the mouse col1a2 gene. Finally, we produced three *COL7A1* constructs for transgenic mice (Figure 1A). They were digested with appropriate restriction enzymes, purified, and introduced into BDF1 oocytes, which were subsequently transplanted into the recipient mice. Founders were bred to wild-type C57BL/6 females. To confirm germline transmission, PCR analyses on genomic DNA were performed (forward, 5′-CTCAGTGGATGTTGCCTTT-3′; reverse, 5′-TAAGAACACAATGTCAGCGG-3′) using specific primers and the following thermal cycling parameters: 94°C for 5 minutes, 94°C for 45 seconds, and 56°C for 45 seconds; followed by 35 cycles at 72°C for 45 seconds and 72°C for 7 minutes. The transgenic (Tg) mice with K14, col1a2, and CMV

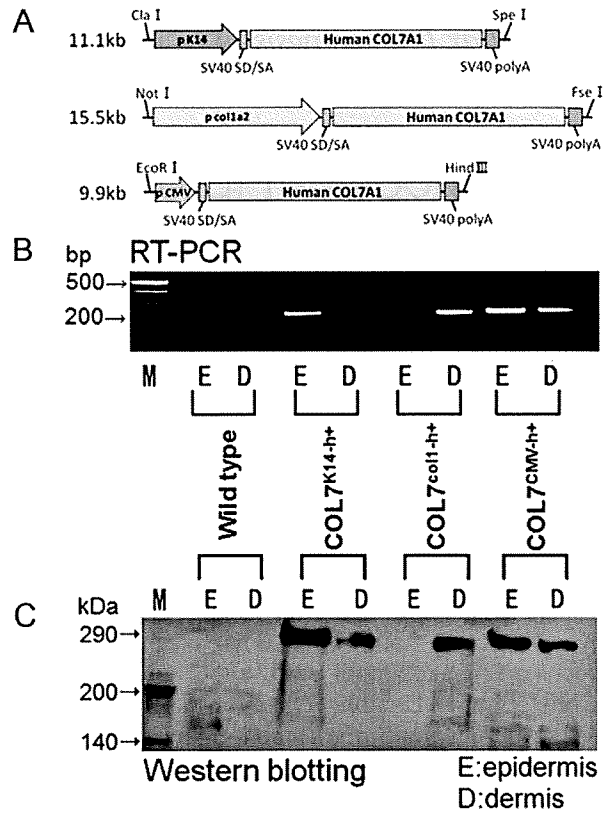

Figure 1. Epidermis- or dermis-specific expression of the human *COL7A1* full-length cDNA in the transgenic mice. **A:** Three expression vectors for transgenic mice were constructed using the promoters of human K14, mouse col1a2, and CMV. The vector contains the SV40 splice donor/splice acceptor (SD/SA) site and the SV40 polyadenylation (polyA) signal. **B:** We obtained epidermis and dermis from the K14Tg mice (COL7$^{K14\text{-}h+}$), col1a2Tg mice (COL7$^{col1\text{-}h+}$), and CMVTg mice (COL7$^{CMV\text{-}h+}$) and then examined human *COL7A1* mRNA expression by RT-PCR analysis. Molecular weight markers (M) are a 100-bp DNA ladder. **C:** Expression of COL7 was also investigated by Western blot analysis using anti-human monoclonal antibody LH7.2. Molecular weight markers are a biotinylated protein ladder.

Table 1. Summary of the Genetically Engineered Mice Involved in This Study

Mouse	Genotype	Phenotype
$COL7^{m-/-}$	Knockout mouse with targeted disruption of the mouse *Col7a1* encoding mouse type VII collagen	RDEB (severe disease phenotype)
$COL7^{m+/-}$	*Col7a1* heterozygous knockout mouse	Clinically normal
$COL7^{K14\text{-}h+}$	Transgenic mouse with human *COL7A1* driven by the human K14 promoter	Clinically normal
$COL7^{col1\text{-}h+}$	Transgenic mouse with human *COL7A1* driven by the promoter of the gene encoding mouse pro-α 2 chain of type I collagen	Clinically normal
$COL7^{CMV\text{-}h+}$	Transgenic mouse with human *COL7A1* driven by the ubiquitous CMV promoter	Clinically normal
$COL7^{m-/-,\ K14\text{-}h+}$	*Col7a1* knockout mouse rescued by human *COL7A1* with the human K14 promoter	Clinically normal
$COL7^{m-/-,\ col1\text{-}h+}$	*Col7a1* knockout mouse rescued by human *COL7A1* with the mouse pro-α 2 chain of type I collagen promoter	Clinically normal
$COL7^{m-/-,\ CMV\text{-}h+}$	*Col7a1* knockout mouse rescued by human *COL7A1* with the CMV promoter	Clinically normal
$COL7^{K14\text{-}\Delta h+}$	Transgenic mouse with mutated human type VII collagen with 7528delG mutation under the human K14 promoter	Clinically normal
$COL7^{m-/-,\ K14\text{-}\Delta h+}$	*Col7a1* knockout mouse with the mutated human type VII collagen with 7528delG	RDEB (moderate disease phenotype)

promoters were designated as K14Tg mice ($COL7^{K14\text{-}h+}$), col1a2Tg mice ($COL7^{col1\text{-}h+}$), and CMVTg mice ($COL7^{CMV\text{-}h+}$), respectively (Table 1).

Transgenic Rescue Experiment

Transgenic mice with different promoters ($COL7^{K14\text{-}h+}$, $COL7^{col1\text{-}h+}$, and $COL7^{CMV\text{-}h+}$) were crossbred to heterozygous *col7a1* knockout mouse ($COL7^{m+/-}$) generated by Heinonen et al[3] to create heterozygous mice carrying human *COL7A1* cDNA. Then these mice were mated again with $COL7^{m+/-}$ mice to obtain a mouse that harbored the human COL7 gene in a *col7a1* knockout background. The resulting transgenic rescue mice, each with either the K14, col1a2, or CMV promoter, were, respectively, designated as $COL7^{m-/-,\ K14\text{-}h+}$, $COL7^{m-/-,\ col1\text{-}h+}$, and $COL7^{m-/-,\ CMV\text{-}h+}$ (Table 1). The rescued mice ($COL7^{m-/-,\ K14\text{-}h+}$, $COL7^{m-/-,\ col1\text{-}h+}$, and $COL7^{m-/-,\ CMV\text{-}h+}$) were analyzed by histopathological, immunofluorescence, and immunoblot analyses as described below. Whole-skin samples from the rescued mice were used for the immunoblot analysis.

RT-PCR and Western Blot Analysis

Mouse skin was obtained from the back of each mouse and incubated with 10 mg/ml dispase for 8 hours at 4°C to separate the epidermis and dermis. The epidermal and dermal sheets were minced, and total RNA was extracted using an RNeasy RNA extraction kit (Qiagen, Hilden, Germany). The cDNA was synthesized with the SuperScript First-Strand Synthesis System for RT-PCR (Invitrogen, Grand Island, NY) and subjected to PCR, using specific primers (forward, 5′-CTCAGTGGATGTTGCCTTTA-3′; reverse, 5′-TAAGAACACAATGTCAGCGG-3′) and the following thermal cycling parameters: 94°C for 5 minutes, 94°C for 1 minute, and 56°C for 1 minute; followed by 35 cycles at 72°C for 1 minute and 72°C for 7 minutes.

For Western blot analysis, the epidermal and dermal sheets were mixed with a protease inhibitor cocktail (Sigma-Aldrich, St. Louis, MO), homogenized, and centrifuged at 15,000 × *g*. The supernatant of each sample was separated on a 5% polyacrylamide gel under reducing conditions. Immunoblotting analysis was performed by incubation with the LH7.2 monoclonal antibody (1:1000) for 18 hours at 4°C and then with secondary goat anti-mouse IgG antibodies conjugated with peroxidase (1:2000) for 1 hour at 37°C. The resultant complexes were processed using the Phototope HRP Western Blot Detection System (Cell Signaling Technology, Beverly, MA) according to the manufacturer's protocol.

Histopathological, Immunofluorescence, Ultrastructural, and Immunoelectron Microscopic Analyses

Mouse skin samples were fixed in 10% formalin neutral buffer solution for paraffin embedding or were immediately frozen in OCT compound and stored at −80°C. Paraffin-embedded sections were cut to 5 μm and stained with H&E solution. Alternatively, the LH7.2 monoclonal antibody against the NC-1 amino-terminal domain of COL7 (Chemicon, Temecula, CA) was used for immunofluorescence staining on frozen sections from tissue samples embedded in OCT compound. The bound antibodies were detected with fluorescein isothiocyanate-conjugated goat anti-mouse IgG antibody (Jackson ImmunoResearch Laboratories, Inc., West Grove, PA). Nuclear counterstaining with propidium iodide was performed in some immunofluorescence labeling experiments.

For electron microscopic examination, skin specimens were fixed in 5% glutaraldehyde, postfixed in 1% osmium tetroxide, and stained en block in uranyl acetate. They were dehydrated in a graded ethanol series and embedded in Araldite 6005. Ultrathin sections were cut and stained with uranyl acetate and lead citrate. The sections were examined with a transmission electron microscope (H-7100; Hitachi, Tokyo, Japan) at 75 kV. For semiquantitative morphometric analysis, the number of anchoring fibrils on electron micrographs was counted and the number of anchoring fibrils per unit length of lamina

densa was estimated as number of anchoring fibrils/1 μm of lamina densa. Minimal anchoring fibril features required for quantification were the presence of an arch structure of fibrils inserted into the dermis from the lamina densa. Twenty electron microscopic sections were examined for each mouse line. For immunoelectron microscopic analysis, skin samples were cryofixed with liquid propane cooled with nitrogen, cryosubstituted at −80°C, and low temperature-embedded at −60°C in Lowicryl K11M resin before undergoing UV polymerization. Ultrathin sections were cut to 90 nm thickness. The LH7.2 monoclonal antibody was used as the primary antibody, and then a goat anti-rabbit IgG 10-nm gold-conjugated secondary antibody was used (Amersham, Poole, UK). The sections were stained with uranyl acetate and lead citrate and examined with a transmission electron microscope.

Transgenic Rescue Experiment with the Human Mutated Gene

We generated a full-length human *COL7A1* cDNA containing the c.7528delG mutation and replaced the normal human *COL7A1* cDNA K14 promoter construct (Figure 1A) with the human mutated *COL7A1* cDNA (c.7528delG). The guanine at 7528 is at the end of the collagenous domain of COL7, and the mutation creates a premature stop codon at 18 bp downstream. The expressed protein is a truncated COL7 lacking the NC-2 domain at the C terminus. Using the same techniques as described above, we produced transgenic mice by microinjection, screening PCR, and germline transmission. The transgenic mice ($COL7^{K14\text{-}\Delta h+}$) were crossbred to heterozygous *col7a1* knockout mouse ($COL7^{m-/-}$). Then these mice ($COL7^{m+/-,\ K14\text{-}\Delta h+}$) were intercrossed to obtain a mouse that harbored the mutated human COL7 gene in a *col7a1* knockout background (Table 1). The rescued mice ($COL7^{m-/-,\ K14\text{-}\Delta h+}$) were analyzed by histopathological, immunofluorescence, and immunoblot analyses as described above.

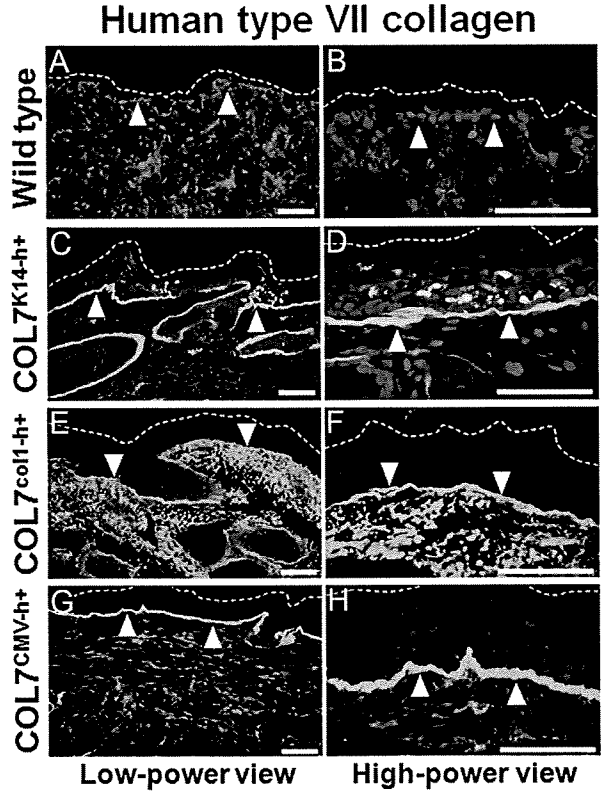

Figure 2. Both epidermis- and dermis-targeted transgene products of human COL7 molecules were precisely localized in the dermoepidermal junction in the transgenic mice. Immunofluorescence staining with the anti-human COL7 monoclonal antibody LH7.2 showed no human COL7 immunolabeling in the dermoepidermal junction of the wild-type mouse skin (**A** and **B**). Skin samples from all three transgenic mouse lines (keratinocyte-targeted K14Tg mice ($COL7^{K14\text{-}h+}$) (**C** and **D**), fibroblast-targeted col1a2Tg mice ($COL7^{col1\text{-}h+}$) (**E** and **F**), and CMVTg mice with ubiquitous COL7 expression ($COL7^{CMV\text{-}h+}$) (**G** and **H**) showed human COL7 linear staining at the epidermal BMZ (**white arrowheads**). $COL7^{K14\text{-}h+}$ mouse skin revealed additional punctate staining in epidermal keratinocytes, and $COL7^{col1\text{-}h+}$ mouse skin showed additional diffuse staining in dermal fibroblasts. Dotted lines demarcate the skin surface. Left column (**A, C, E,** and **G**), low-power view; right column (**B, D, F,** and **H**), high-power view. Human COL7 immunolabeling, green (fluorescein isothiocyanate); nuclear stain, red (propidium iodide). Scale bars = 50 μm.

Results

Generation of Transgenic Mice Showing Keratinocyte- or Fibroblast-Targeted Expression of Human COL7

To allow selective expression of human *COL7A1* in epidermal keratinocytes or in dermal fibroblasts, we used human K14 and mouse col1a2 promoters, which have been shown to specify epidermal and dermal expression in mice, respectively.[10,11] The mice with K14 or col1a2 promoters were designated as K14Tg mice ($COL7^{K14\text{-}h+}$) and col1a2Tg mice ($COL7^{col1\text{-}h+}$), respectively (Figure 1A). In addition, the ubiquitous CMV promoter was used to generate transgenic mice with both epidermal and dermal expression (CMVTg mice: $COL7^{CMV\text{-}h+}$) (Figure 1A). To demonstrate tissue-specific expression, we obtained epidermis and dermis from the mice and determined *COL7A1* mRNA expression by RT-PCR analysis using primers specific for human transcripts. The results show that $COL7^{K14\text{-}h+}$ mice *COL7A1* mRNA expression is restricted to the epidermis and mRNA expression of *COL7A1* in $COL7^{col1\text{-}h+}$ mice is restricted to the dermis. Expression of epidermal and dermal *COL7A1* mRNA was detected in $COL7^{CMV\text{-}h+}$ mice (Figure 1B). Western blot analysis also shows epidermal or dermal expression mostly consistent with the specific promoters, except for a weak COL7 band detected in the dermal component from $COL7^{K14\text{-}h+}$ mice (Figure 1C). A small amount of COL7 secreted by epidermal keratinocytes moves into the dermal side. The weak COL7 band in the dermal component from $COL7^{K14\text{-}h+}$ mice probably reflects the translocated COL7 peptides.

Immunofluorescence study using LH7.2 anti-human COL7 monoclonal antibody showed the linear epidermal

BMZ staining in all three transgenic mice lines (Figure 2, A and B, wild-type; Figure 2, C and D, $COL7^{K14\text{-}h+}$; Figure 2, E and F, $COL7^{col1\text{-}h+}$; and Figure 2, G and H, $COL7^{CMV\text{-}h+}$). $COL7^{K14\text{-}h+}$ revealed additional punctate staining in epidermal keratinocytes (Figure 2, C and D), and $COL7^{col1\text{-}h+}$ revealed additional diffuse staining in dermal fibroblasts (Figure 2, E and F). In the course of the transgenic mouse experiments, we obtained several lines of mice and were able to generate offspring in $COL7^{K14\text{-}h+}$, $COL7^{col1\text{-}h+}$, and $COL7^{CMV\text{-}h+}$ lineages. In each transgenic line, we selected the mouse with the most robust *COL7A1* expression for the subsequent rescue experiments.

Keratinocyte-/Fibroblast-Targeted Transgenic Rescue of COL7 Knockout Mice

Col7a1 knockout mice ($COL7^{m-/-}$) exhibit a severe, recessive DEB phenotype, and these mice die within a few days after birth. We initiated transgenic rescue experiments of $COL7^{m-/-}$ mice by mating $COL7^{m+/-}$, $COL7^{col1\text{-}h+}$, or $COL7^{CMV\text{-}h+}$ transgenic mice. After further crossing, transgenic mice on a *col7a1* knockout background ($COL7^{m-/-,\ K14\text{-}h+}$, $COL7^{m-/-,\ col1\text{-}h+}$, and $COL7^{m-/-,\ CMV\text{-}h+}$) were generated, and they showed expression of human COL7 under the different promoters. All three different rescued mice ($COL7^{m-/-,\ K14\text{-}h+}$,

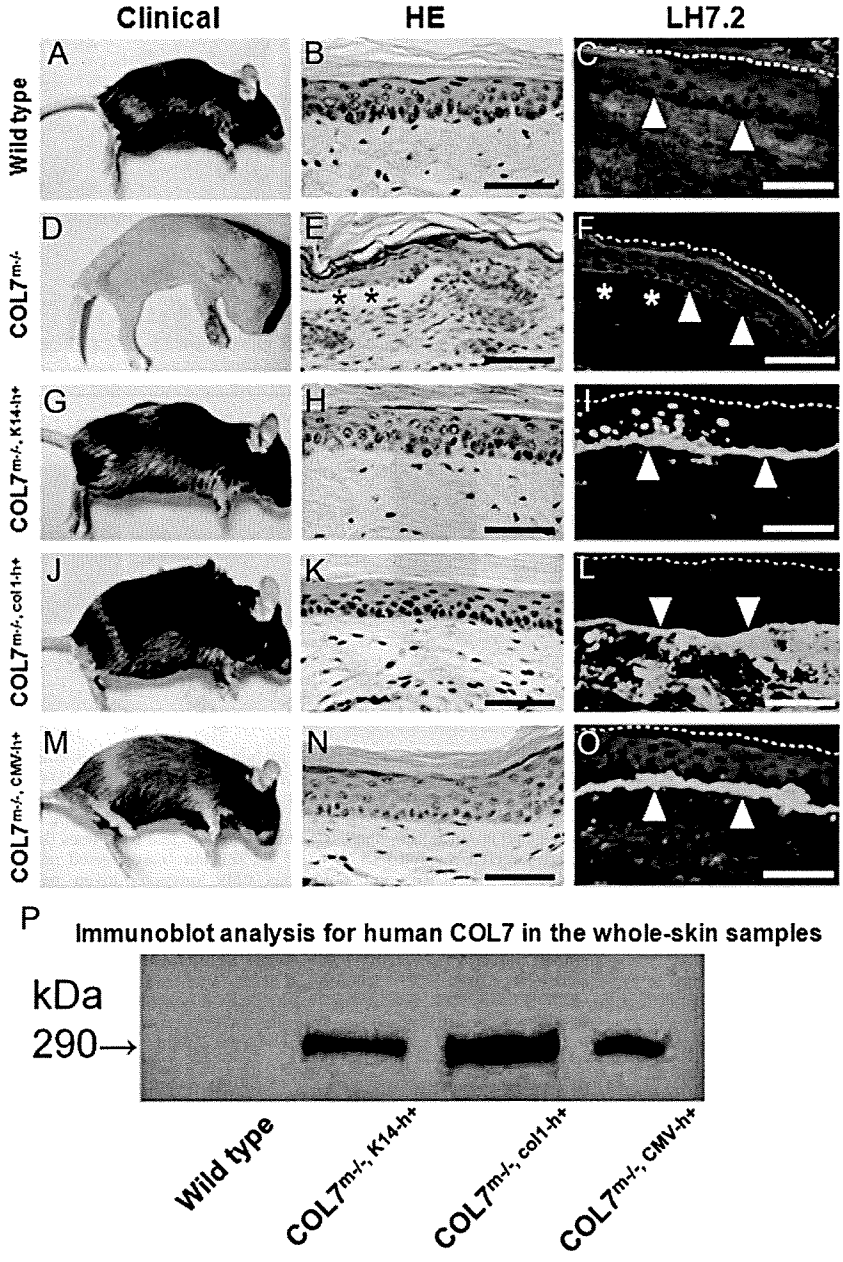

Figure 3. Keratinocyte-/fibroblast-targeted human *COL7A1* transgene can rescue COL7 knockout mice. A wild-type mouse showed a normal phenotype (**A**) and intact dermoepidermal junction (**B**) without human COL7 expression (**C, white arrowheads**). A $COL7^{m-/-}$ mouse had a severe DEB phenotype (**D**) and apparent dermoepidermal separation (**E, asterisks**) without human COL7 (**F, white arrowheads**). All three rescued mice (keratinocyte-targeted rescued $COL7^{m-/-,\ K14\text{-}h+}$ [**G–I**], fibroblast-targeted rescued $COL7^{m-/-,\ col1\text{-}h+}$ [**J–L**]), and ubiquitous CMV promoter-driven rescued $COL7^{m-/-,\ CMV\text{-}h+}$ [**M-O**]) showed no DEB phenotype (**G, J,** and **M**) and an intact dermoepidermal junction (**H, K,** and **N**). Immunofluorescence labeling revealed human COL7 in the basement membrane zone (**white arrowheads**) in skin sections from all three rescued mice (**I, L,** and **O**). Skin from the keratinocyte-targeted rescued $COL7^{m-/-,\ K14\text{-}h+}$ mouse showed additional punctate staining in epidermal keratinocytes (**I**), and skin from the fibroblast-targeted rescued $COL7^{m-/-,\ col1\text{-}h+}$ mouse revealed additional diffuse staining in dermal fibroblasts (**L**). Immunofluorescence staining with anti-human COL7 monoclonal antibody, LH7.2, fluorescein isothiocyanate, green (**C, F, I, L,** and **O**). **White arrowheads**, basement membrane zone; **asterisks,** a blister cavity. Dotted lines demarcate the skin surface. Scale bars = 50 μm. **P:** Immunoblot analysis for human COL7 in the whole-skin samples from the wild-type and the three rescued mouse lines. Human COL7 protein expression was confirmed in the whole skin of all three lines of rescued mice ($COL7^{m-/-,\ K14\text{-}h+}$, $COL7^{m-/-,\ col1\text{-}h+}$, and $COL7^{m-/-,\ CMV\text{-}h+}$) but not in the wild-type mice. From the density of immunoblot bands, amounts of human COL7 expressed in the whole-skin samples were the greatest in $COL7^{m-/-,\ col1\text{-}h+}$ line among the three lines of rescued mice. The other two rescued lines, $COL7^{m-/-,\ CMV\text{-}h+}$ and $COL7^{m-/-,\ K14\text{-}h+}$, expressed roughly similar amounts of human COL7.

$COL7^{m-/-,\ col1\text{-}h+}$, and $COL7^{m-/-,\ CMV\text{-}h+}$) showed normal appearance at birth, and no DEB phenotype was observed (Figure 3, A, D, G, J, and M). Remarkably, all of the rescued mice ($COL7^{m-/-,\ K14\ hours\text{-}+}$, $COL7^{m-/-,\ col1\text{-}h+}$, and $COL7^{m-/-,\ CMV\text{-}h+}$) exhibited reproductive ability despite the fact that the original $COL7^{m-/-}$ mice were lethal and unable to reproduce. All of these rescued mice had at least a 1-year lifespan, similar to that of wild-type mice. We could not detect any blistering, even on a histological scale (Figure 3, B, E, H, K, and N) and immunofluorescence study using LH7.2 showed positive linear staining of COL7 along the BMZ in all three lines of rescued mice ($COL7^{m-/-,\ K14\text{-}h+}$, $COL7^{m-/-,\ col1\text{-}h+}$, and $COL7^{m-/-,\ CMV\text{-}h+}$) (Figure 3, C, F, I, L, and O). The pattern of positive staining was essentially identical to that in the respective original transgenic mice (Figure 2, A–H). Immunoblot analysis for human COL7 in the whole-skin samples from the transgenic rescued mice confirmed that human COL7 protein was expressed in the whole skin of all three lines of rescued mice ($COL7^{m-/-,\ K14\text{-}h+}$, $COL7^{m-/-,\ col1\text{-}h+}$, and $COL7^{m-/-,\ CMV\text{-}h+}$) (Figure 3P). The thicknesses of the immunoblot bands suggested that, in the whole-skin samples, $COL7^{m-/-,\ col1\text{-}h+}$ expressed the most human COL7 among the three lines of rescued mice, and the other two rescued lines, $COL7^{m-/-,\ CMV\text{-}h+}$ and $COL7^{m-/-,\ K14\text{-}h+}$, produced similarly less human COL7.

Electron microscopy of the skin showed newly formed anchoring fibrils in the sublamina densa area in all of the rescued mice ($COL7^{m-/-,\ K14\text{-}h+}$, $COL7^{m-/-,\ col1\text{-}h+}$, and $COL7^{m-/-,\ CMV\text{-}h+}$) (Figure 4, A, C, E, G, and I). Semiquantitative morphometric analysis of numbers of anchoring fibrils on electron microscopic images revealed the anchoring fibril density in each mouse line as follows (mean ± SD number of anchoring fibrils/μm): wild-type $COL7^{m+/+}$, 3.41 ± 0.43; $COL7^{m-/-}$, 0.00 ± 0.00; $COL7^{m-/-,\ K14\text{-}h+}$, 2.60 ± 0.46; $COL7^{m-/-,\ col1\text{-}h+}$, 2.85 ± 0.39; and $COL7^{m-/-,\ CMV\text{-}h+}$, 3.09 ± 0.30 (Figure 4K). Immunoelectron microscopic analysis of the skin obtained from each line of rescued mice revealed that LH7.2-labeled gold particles were localized in the lamina densa of the BMZ (Figure 4, B, D, F, H, and J). The epitopes of LH7.2 monoclonal antibody are known to react to the NC-1 domain of COL7, which is known to be located along the lamina densa.[12] The results suggest that COL7 synthesized from transgenes functioned correctly, irrespective of whether it originated from fibroblasts or from keratinocytes.

Generation of an Exact DEB Model Mice Carrying Human COL7A1 Mutation

In the course of cloning experiments, we obtained several mutant *COL7A1* clones that demonstrated abnormal *COL7A1* expression. Subsequent sequence analysis revealed that one of those clones had a c.7528delG mutation in the *COL7A1* cDNA. We then constructed an expression vector of the mutated *COL7A1* under the K14 promoter and generated the transgenic mice. Next, we crossed these mutant $COL7^{K14\text{-}\Delta h+}$ transgenic mice with $COL7^{m+/-}$ het-

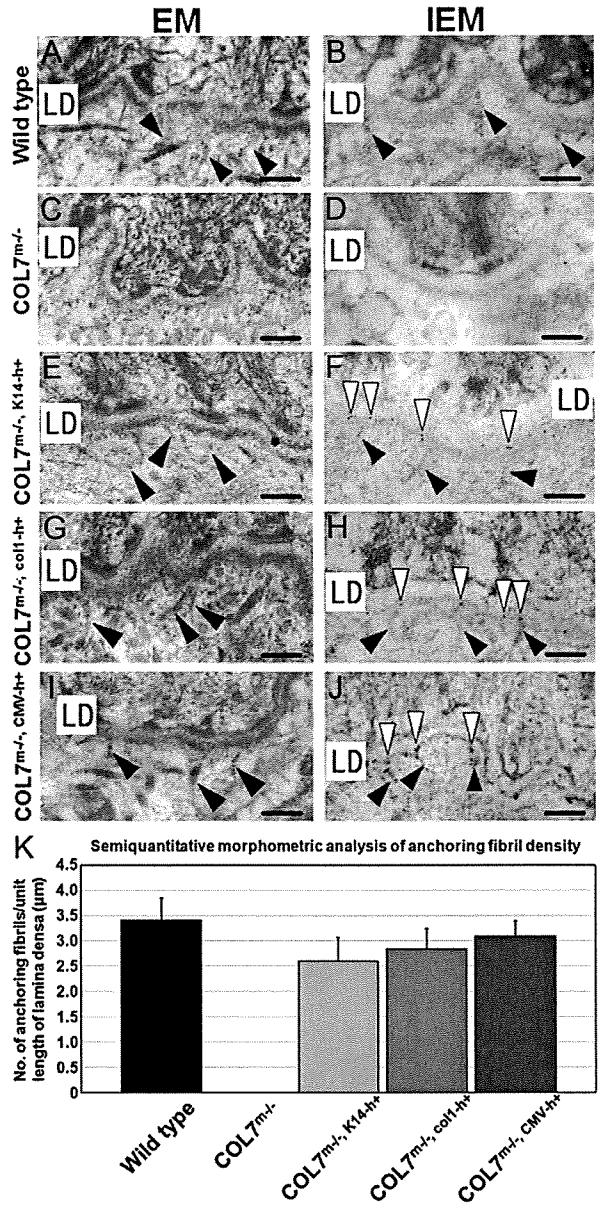

Figure 4. Transgene products, which are human COL7 molecules, correctly form anchoring fibrils in the rescued mice. Electron microscopy (EM) (**A, C, E, G,** and **I**) demonstrated intact anchoring fibrils (**black arrowheads**) in the sublamina densa area in a wild-type mouse (**A**). In contrast, the $COL7^{m-/-}$ mouse had no anchoring fibrils (**C**). In all three rescued mice lines (keratinocyte-targeted rescued $COL7^{m-/-,\ K14\text{-}h+}$ [**E**], fibroblast-targeted rescued $COL7^{m-/-,\ col1\text{-}h+}$ [**G**], and ubiquitous CMV promoter-driven rescued $COL7^{m-/-,\ CMV\text{-}h+}$ [**I**]), anchoring fibril formation was restored in the sublamina densa area (**black arrowheads**). Immunoelectron microscopy (IEM) using LH7.2 (**B, D, F, H,** and **J**) revealed no human COL7 labeling (gold particle) in intact anchoring fibrils (**black arrowheads**) of a wild-type mouse (**B**). The $COL7^{m-/-}$ mouse had neither anchoring fibrils nor human COL7 labeling (**D**). Human COL7 (immunogold particles, **white arrowheads**) was localized in the lamina densa of the basement membrane zone in all three rescued mice: keratinocyte-targeted rescued $COL7^{m-/-,\ K14\text{-}h+}$ (**F**), fibroblast-targeted rescued $COL7^{m-/-,\ col1\text{-}h+}$ (**H**), and ubiquitous CMV promoter-driven rescued $COL7^{m-/-,\ CMV\text{-}h+}$ (**J**). **Black arrowheads**, anchoring fibrils; **white arrowheads**, human COL7 labeling (immunogold particles); LD, lamina densa. Scale bars = 200 nm. **K:** Semiquantitative morphometric analysis of anchoring fibril density. Anchoring fibril density was highest in ubiquitous CMV promoter-driven rescued $COL7^{m-/-,\ CMV\text{-}h+}$, second highest in fibroblast-targeted rescued $COL7^{m-/-,\ col1\text{-}h+}$, and lowest in keratinocyte-targeted rescued $COL7^{m-/-,\ K14\text{-}h+}$ mice, among the three lines of rescued mice, although no statistically significant difference was observed between any combination of the three lines.

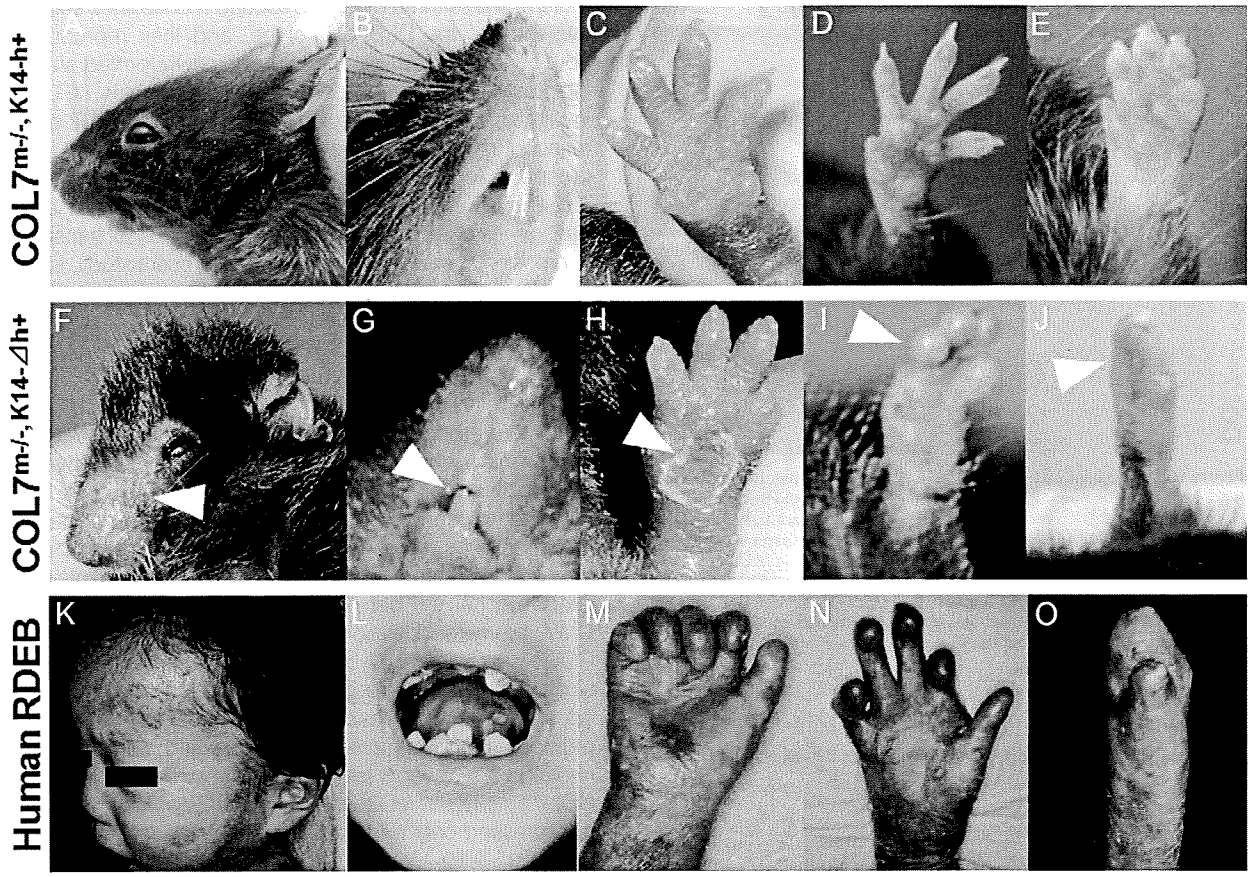

Figure 5. DEB model mice carrying a human *COL7A1* mutation precisely reproduce the DEB phenotype. **A–E:** *Col7a1* knockout mice rescued by full-length human *COL7A1* ($COL7^{m-/-, K14-h+}$) are clinically normal. Forepaws of $COL7^{m-/-, K14-h+}$ mice at 14 days (**C**), 30 days (**D**), and 60 days of age (**E**). **F–J:** *Col7a1* knockout mice rescued by mutated human *COL7A1* ($COL7^{m-/-, K14-\Delta h+}$) show gradual development of mild alopecia (**F**), yellowish dental caries (**G**), and fusion of the paw digits (**I** and **J**), corresponding to the clinical phenotype of human DEB. (**K** and **M:** A 2-year-old male patient harboring *COL7A1* mutations, c.[5818delC] + p.[Gly2623Ser].[13] **L:** A 10-year-old female patient whose mutations were unidentified. The diagnosis was confirmed by ultrastructural observation and immunofluorescence studies. **N:** A 15-year-old male patient with p.[Gly2576Arg] + [Glu2858X].[14] **O:** A 51-year-old female patient harboring p.[Gly1815Arg] + c.[5818delC].[15]) Forepaws of $COL7^{m-/-, K14-\Delta h+}$ mice were documented at 14 days (**H,** scarring), 30 days (**I,** mild fusion), and 60 days of age (**J,** complete fusion) (**white arrowheads**).

erozygous mice to obtain mutant $COL7^{m+/-, K14-\Delta h+}$ mice. We then performed transgenic rescue experiments by intercrossing these mice ($COL7^{m+/-, K14-\Delta h+}$) and obtained $COL7^{m-/-, K14-\Delta h+}$ mice. Immunoblot analysis on epidermal extract samples from $COL7^{m-/-, K14-\Delta h+}$ mice confirmed the expression of short, truncated human COL7 derived from mutant COL7A1 (data not shown).

From birth, the $COL7^{m-/-, K14-\Delta h+}$ mice were indistinguishable from their wild-type littermates and showed no blistering, not even on the paws, despite the fact that hemorrhagic bullae are always found in $COL7^{m-/-}$ mice. The growth of the human mutant-rescued mice ($COL7^{m-/-, K14-\Delta h+}$) was retarded, however, compared with that of their wild-type littermates. Interestingly, the $COL7^{m-/-, K14-\Delta h+}$ mice gradually developed the DEB phenotype, including nail dystrophy, scarring on the paws, fusion of the digits, yellowish dental caries, and mild alopecia, characteristic features of human RDEB (Figure 5, K–O).[13–15] It was difficult to distinguish the alopecia seen in the $COL7^{m-/-, K14-\Delta h+}$ mice from barbarism only from clinical appearance. However, the penetration of the alopecia is almost 100% in the $COL7^{m-/-, K14-\Delta h+}$ mice, whereas only a few wild-type littermates that were kept in the same condition showed barbarism. Thus, this alopecia was considered to be a feature specific to the $COL7^{m-/-, K14-\Delta h+}$ mice. These DEB clinical phenotypic manifestations were evident at 2 months of age (Figure 5, F–J). The clinical course of the forepaws showed a phenotype that is very characteristic of DEB. The $COL7^{m-/-, K14-\Delta h+}$ mice showed no blistering at birth, yet there was scarring of the forepaws 2 weeks later (Figure 5H). By 1 month, the paws had become mildly fused (Figure 5I), and complete fusion of paws (mitten deformity) was observed at 2 months (Figure 5J). The growth of the full-length human gene-rescued mice ($COL7^{m-/-, K14-h+}$) did not differ notably from that of the wild-type mice (Figure 5, A–E). During histopathological investigation, although clinically detectable blistering was not observed, we demonstrated microblistering along the dermal-epidermal junction in these mice ($COL7^{m-/-, K14-\Delta h+}$) by histopathological analysis (Figure 6, A and C). Immunofluorescence analysis showed immunoreactivity of human COL7 in the BMZ of the $COL7^{m-/-, K14-\Delta h+}$ mice (Figure 6, B and D). Most of the human mutant mice had about a 6-month lifespan (Figure 5,

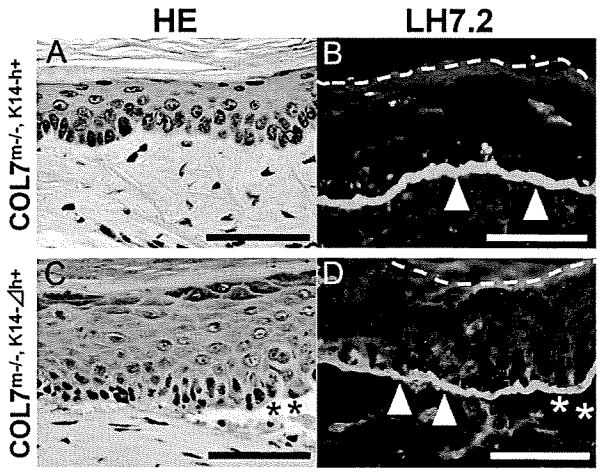

Figure 6. The humanized DEB model mouse shows subepidermal blistering with deposition of mutant human COL7 at the dermoepidermal junction. **A:** A $COL7^{m-/-,\ K14\text{-}h+}$ mouse has histopathologically normal skin. **C:** A $COL7^{m-/-,\ K14\text{-}\Delta h+}$ mouse shows subepidermal blistering (**asterisks**). **B** and **D:** Immunofluorescence study using anti-human COL7 antibody, LH7.2, reveals positive linear staining within the BMZ (**white arrowheads**), corresponding to normal and mutant human COL7 in a $COL7^{m-/-,\ K14\text{-}h+}$ mouse and a $COL7^{m-/-,\ K14\text{-}\Delta h+}$ mouse, respectively (**asterisks** indicate a blister cavity). Dotted lines demarcate the skin surface. Scale bars = 50 μm.

F-J). Thus, the clinical manifestations of human DEB were reproduced in the mouse by corrective transfer of human mutated *COL7A1* gene.

Discussion

COL7 is a major component of anchoring fibril loop structures beneath the epidermal basement membrane.[12,16] Previous studies have indicated that epidermal keratinocytes are the primary source of COL7 in developing human skin.[5,6] Thus, epidermal keratinocytes have been the main focus in the development of corrective gene therapies for DEB caused by *COL7A1* mutations. However, we recently showed that gene-transferred fibroblasts can supply a larger proportion of COL7 to the new dermal-epidermal junction as efficiently as gene-transferred keratinocytes.[17] Moreover, fibroblasts are more robust and less susceptible to growth arrest and differentiation than are epidermal keratinocytes.[6] Our study is are the first *in vivo* study to show that keratinocytes and fibroblasts, through direct comparative studies, are both feasible targets for DEB gene therapy. In addition, this study can be extended to other basement membrane proteins, and fibroblasts may provide those proteins from the dermis toward the epidermis.

We first generated several transgenic mice with COL7 expression under the control of each of the following promoters: K14, col1a2, and CMV. We have shown that COL7 expression from either keratinocytes or dermal fibroblasts can be fully integrated into the epidermal BMZ *in vivo*. We have also shown that expression of COL7 by either keratinocytes or fibroblasts can successfully rescue $COL7^{m-/-}$ mice.[3] Consequently, the rescued mice ($COL7^{m-/-,\ K14\text{-}h+}$, $COL7^{m-/-,\ col1\text{-}h+}$, and $COL7^{m-/-,\ CMV\text{-}h+}$) show expression of human COL7 under the control of the different promoters. These three different rescued mouse lines show no evidence of the DEB phenotype, and their reproductive ability was restored. Ultrastructurally, newly formed anchoring fibrils were present, and the NC-1 domain of COL7 localized precisely in the lamina densa of the BMZ in the rescued mice. Collectively, these results provide future prospects for corrective gene therapy for DEB.

Generally speaking, the nature of promoters used in transgenes does not always define the amount of transgene expression in transgenic mice. In the present study, immunofluorescence and immunoblot analysis suggested that fibroblast-targeted rescued $COL7^{m-/-,\ col1\text{-}h+}$ mice expressed more human COL7 than that expressed in ubiquitous CMV promoter-driven rescued $COL7^{m-/-,\ CMV\text{-}h+}$ mice and keratinocyte-targeted rescued $COL7^{m-/-,\ K14\text{-}h+}$ mice. Interestingly, in contrast, semiquantitative morphometric analysis of anchoring fibril density revealed that anchoring fibril density was highest in the ubiquitous CMV promoter-driven rescued $COL7^{m-/-,\ CMV\text{-}h+}$ mice, among the three lines of rescued mice, although no statistically significant difference was confirmed. We cannot explain the exact mechanism behind this discrepancy. In ubiquitous CMV promoter-driven rescued $COL7^{m-/-,\ CMV\text{-}h+}$ skin, COL7 is produced by both fibroblasts and keratinocytes, similar to the physiological manner of COL7 expression. Thus, we speculate that, in $COL7^{m-/-,\ CMV\text{-}h+}$ skin, COL7 peptides might be more efficiently assembled to form anchoring fibrils, even if less protein is expressed than in the $COL7^{m-/-,\ col1\text{-}h+}$ or $COL7^{m-/-,\ K14\text{-}h+}$ skin in which COL7 is expressed only by fibroblasts or keratinocytes, respectively.

The mice developed in this study can also provide a useful model for immunobullous diseases involving COL7. Recently, we succeeded in generating a bullous pemphigoid model.[18] Passive transfer of bullous pemphigoid autoantibodies into wild-type mice has failed to induce skin lesions, because of differences between humans and mice in the amino acid sequence of the pathogenic epitope of the autoantigen, COL7.[19] We injected the patients' autoantibody into murine COL7 knockout mice that had been rescued by the expression of the human autoantigen. This resulted in successful reactions by autoantigens and autoantibodies, thereby producing the bullous pemphigoid phenotype. Epidermolysis bullosa acquisita is an autoimmune blistering disorder, and the patients' autoantibodies react to COL7. Therefore, the rescued mice with humanized COL7 that we produced should be useful in future research on epidermolysis bullosa acquisita as well.

Another interesting aspect of the present study is that we were able to develop $COL7^{K14\text{-}\Delta h+}$ transgenic mice with human *COL7A1* cDNA containing the mutation c.7528delG. The $COL7^{K14\text{-}\Delta h+}$ transgenic mice and the $COL7^{m-/-,\ K14\text{-}\Delta h+}$ rescued mice showed positive human COL7 staining at the BMZ, indicating that COL7 without the NC-2 domain can still form a triple helix and be secreted by keratinocytes. The characteristic component of all collagens is the triple helix formed by three subunits, and its assembly is based on the repetition of the Gly-X-Y repeats. It has been suggested that a zipper-like mechanism of triple helix formation starts from the C

terminus toward the N terminus in collagens I and IV[20–22] and from the N-terminal to the C-terminal direction in epidermal type XVII collagen.[23] Our experiments using the genetically engineered mouse model suggest that the N- to C-terminal mechanism of triple helix formation is also possible for COL7. However, lack of the NC-2 domain, which is critical for antiparallel-dimer formation, might cause partial and weak immunoreactivity of human COL7 in the BMZ of $COL7^{m-/-,\ K14\text{-}\Delta h+/+}$ mice. This study demonstrates the importance of the NC-2 domain in COL7 formation and assembly *in vivo*.

Of importance, we have generated a mouse model of DEB that allows for long-term studies that were not possible with the previously generated neonatal lethal $COL7^{m-/-}$ *col7a1* knockout mice. A surviving DEB mouse model (the mouse COL7 hypomorphic mouse) that was recently reported expresses mouse COL7 at approximately 10% of normal levels.[4] These mice could survive longer than *Col7a1* knockout mouse ($COL7^{m-/-}$) and present clinical phenotypes (mitten hands and feet) similar to those of human DEB. The phenotypes of these model mice were produced from the gene-engineered mouse COL7 gene using a hypomorphic technique. These mice had a high mortality rate (67%) within 28 days without a change to a liquid diet consisting of infant milk. On the contrary, our novel mouse models of RDEB were generated by completely different methodology using a mutated human *COL7A1* gene, and the mouse could survive longer without use of a liquid diet. Surprisingly, our original DEB model mouse is very similar to humans not only in terms of clinical manifestations but also in terms of the genetic background. In fact, the $COL7^{m-/-,\ K14\text{-}\Delta h+}$ mice demonstrated nail dystrophy, scarring on the paws, fusion of the digits, yellowish dental caries, and mild alopecia, even in the absence of overt blistering. The previous *col7a1* knockout $COL7^{m-/-}$ mice developed spontaneous blistering soon after birth and died within several days.[3] Thus, $COL7^{m-/-}$ mice have not been available for long-term experiments. In this study, the production of rescued mice with mutated *COL7A1* ($COL7^{m-/-,\ K14\text{-}\Delta h+}$) has given us a surviving model of DEB. This model has great potential for future research into the pathomechanisms of DEB, wound healing, the development of squamous cell carcinomas, and the development of molecular therapies for patients with DEB.

Although we used cDNA with the mutation c.7528delG, which causes a premature stop termination codon (PTC), the consequences of the PTC mutation in the *COL7A1* cDNA are different from those in the *COL7A1* gene. Genomic PTC mutations are subject to nonsense-mediated mRNA decay, resulting in mRNA degradation in some instances. In the literature, genomic PTC mutations in *COL7A1* were previously reported to result in nonsense-mediated mRNA decay and absence of COL7 protein synthesis in severe generalized cases of RDEB.[24,25] Whether a genomic PTC mutation leads to nonsense-mediated mRNA decay depends on the mutation site.[26] In contrast, the PTC mutation in cDNA does not lead to mRNA decay and is thought to generate a truncated protein. In fact, we confirmed the expression of human COL7 derived from human mutant *COL7A1* in the $COL7^{m-/-,\ K14\text{-}\Delta h+}$ mice by immunoblot analysis (data not shown) and immunofluorescence staining (Figure 6D) in the present study. Approximately 300 distinct *COL7A1* mutations have been identified in patients with DEB around the world, and the clinical features, severity, prognosis, and response to treatment vary depending on the specific mutation.[15,24,27–31] Our understanding of how specific mutations produce differing clinical presentations and prognoses is limited. We believe that our systems have the advantage of being able to use human genes. Because the COL7 gene is almost 30 kb in size, introduction of the gene with PTC mutation might be impractical. However, if we generate the same mouse models with the patient-specific missense mutations in the cDNA or with the patient-specific PTC mutation in partial genomic DNA, which was inserted in the cDNA, then they might be useful for evaluating the prognosis of each patient with a certain mutation and for developing a mutation-specific treatment. This strategy could be extended to the development of therapies tailored to other, currently intractable inherited diseases.

Acknowledgments

We thank Ms. Akari Nagasaki and Ms. Shizuka Miyakoshi for their technical assistance.

References

1. Fine JD, Eady RA, Bauer EA, Bauer JW, Bruckner-Tuderman L, Heagerty A, Hintner H, Hovnanian A, Jonkman MF, Leigh I, McGrath JA, Mellerio JE, Murrell DF, Shimizu H, Uitto J, Vahlquist A, Woodley D, Zambruno G: The classification of inherited epidermolysis bullosa (EB): Report of the Third International Consensus Meeting on Diagnosis and Classification of EB. J Am Acad Dermatol 2008, 58:931–950
2. Uitto J, Pulkkinen L: Molecular genetics of heritable blistering disorders. Arch Dermatol 2001, 137:1458–1461
3. Heinonen S, Männikkö M, Klement JF, Whitaker-Menezes D, Murphy GF, Uitto J: Targeted inactivation of the type VII collagen gene (Col7a1) in mice results in severe blistering phenotype: a model for recessive dystrophic epidermolysis bullosa. J Cell Sci 1999, 112:3641–3648
4. Fritsch A, Loeckermann S, Kern JS, Braun A, Bösl MR, Bley TA, Schumann H, von Elverfeldt D, Paul D, Erlacher M, von Rautenfeld DB, Hausser I, Fässler R, Bruckner-Tuderman L: A hypomorphic mouse model of dystrophic epidermolysis bullosa reveals mechanisms of disease and response to fibroblast therapy. J Clin Invest 2008, 118:1669–1679
5. Ryynänen J, Sollberg S, Parente MG, Chung LC, Christiano AM, Uitto J: Type VII collagen gene expression by cultured human cells and in fetal skin: abundant mRNA and protein levels in epidermal keratinocytes. J Clin Invest 1992, 89:163–168
6. Goto M, Sawamura D, Ito K, Abe M, Nishie W, Sakai K, Shibaki A, Akiyama M, Shimizu H: Fibroblasts show more potential as target cells than keratinocytes in COL7A1 gene therapy of dystrophic epidermolysis bullosa. J Invest Dermatol 2006, 126:766–772
7. Ortiz-Urda S, Lin Q, Green CL, Keene DR, Marinkovich MP, Khavari PA: Injection of genetically engineered fibroblasts corrects regenerated human epidermolysis bullosa skin tissue. J Clin Invest 2003, 111:251–255
8. Woodley DT, Krueger GG, Jorgensen CM, Fairley JA, Atha T, Huang Y, Chan L, Keene DR, Chen M: Normal and gene-corrected dystrophic epidermolysis bullosa fibroblasts alone can produce type VII collagen at the basement membrane zone. J Invest Dermatol 2003, 121:1021–1028
9. Wong T, Gammon L, Liu L, Mellerio JE, Dopping-Hepenstal PJ, Pacy J, Elia G, Jeffery R, Leigh IM, Navsaria H, McGrath JA: Potential of

fibroblast cell therapy for recessive dystrophic epidermolysis bullosa. J Invest Dermatol 2008, 128:2179–2189
10. Shibaki A, Sato A, Vogel JC, Miyagawa F, Katz SI: Induction of GVHD-like skin disease by passively transferred $CD8^+$ T-cell receptor transgenic T cells into keratin 14-ovalbumin transgenic mice. J Invest Dermatol 2004, 123:109–115
11. Denton CP, Zheng B, Shiwen X, Zhang Z, Bou-Gharios G, Eberspaecher H, Black CM, de Crombrugghe B: Activation of a fibroblast-specific enhancer of the proalpha2(I) collagen gene in tight-skin mice. Arthritis Rheum 2001, 44:712–722
12. Shimizu H, Ishiko A, Masunaga T, Kurihara Y, Sato M, Bruckner-Tuderman L, Nishikawa T: Most anchoring fibrils in human skin originate and terminate in the lamina densa. Lab Invest 1997, 76:753–763
13. Sawamura D, Mochitomi Y, Kanzaki T, Nakamura H, Shimizu H: Glycine substitution mutations by different amino acids at the same codon in *COL7A1* cause different modes of dystrophic epidermolysis bullosa inheritance. Br J Dermatol 2006, 155:834–837
14. Shimizu H, McGrath JA, Christiano AM, Nishikawa T, Uitto J: Molecular basis of recessive dystrophic epidermolysis bullosa: genotype/phenotype correlation in a case of moderate clinical severity. J Invest Dermatol 1996, 106:119–124
15. Sawamura D, Goto M, Yasukawa K, Sato-Matsumura K, Nakamura H, Ito K, Nakamura H, Tomita Y, Shimizu H: Genetic studies of 20 Japanese families of dystrophic epidermolysis bullosa. J Hum Genet 2005, 50:543–546; erratum in J Hum Genet 2006, 51:839)
16. Uitto J, Chung-Honet LC, Christiano AM: Molecular biology and pathology of type VII collagen. Exp Dermatol 1992, 1:2–11
17. Woodley DT, Keene DR, Atha T, Huang Y, Ram R, Kasahara N, Chen M: Intradermal injection of lentiviral vectors corrects regenerated human dystrophic epidermolysis bullosa skin tissue in vivo. Mol Ther 2004, 10:318–326
18. Nishie W, Sawamura D, Goto M, Ito K, Shibaki A, McMillan JR, Sakai K, Nakamura H, Olasz E, Yancey KB, Akiyama M, Shimizu H: Humanization of autoantigen. Nat Med 2007, 13:378–383
19. Liu Z, Diaz LA, Troy JL, Taylor AF, Emery DJ, Fairley JA, Giudice GJ: A passive transfer model of the organ-specific autoimmune disease, bullous pemphigoid, using antibodies generated against the hemidesmosomal antigen. BP180 J Clin Invest 1993, 92:2480–2488
20. Engel J, Prockop DJ: The zipper-like folding of collagen triple helices and the effects of mutations that disrupt the zipper. Annu Rev Biophys Biophys Chem 1991, 20:137–152
21. Beck K, Boswell BA, Ridgway CC, Bächinger HP: Triple helix formation of procollagen type I can occur at the rough endoplasmic reticulum membrane. J Biol Chem 1996, 271:21566–21573
22. Söder S, Pöschl E: The NC1 domain of human collagen IV is necessary to initiate triple helix formation. Biochem Biophys Res Commun 2004, 325:276–280
23. Areida SK, Reinhardt DP, Muller PK, Fietzek PP, Kowitz J, Marinkovich MP, Notbohm H: Properties of the collagen type XVII ectodomain: evidence for N- to C-terminal triple helix folding. J Biol Chem 2001, 276:1594–1601
24. Hilal L, Rochat A, Duquesnoy P, Blanchet-Bardon C, Wechsler J, Martin N, Christiano AM, Barrandon Y, Uitto J, Goossens M, Hovnanian A: A homozygous insertion-deletion in the type VII collagen gene (COL7A1) in Hallopeau-Siemens dystrophic epidermolysis bullosa. Nat Genet 1993, 5:287–293
25. Hovnanian A, Rochat A, Bodemer C, Petit E, Rivers CA, Prost C, Fraitag S, Christiano AM, Uitto J, Lathrop M, Barrandon Y, de Prost Y: Characterization of 18 new mutations in COL7A1 in recessive dystrophic epidermolysis bullosa provides evidence for distinct molecular mechanisms underlying defective anchoring fibril formation. Am J Hum Genet 1997, 61:599–610
26. Lejeune F, Maquat LE: Mechanistic links between nonsense-mediated mRNA decay and pre-mRNA splicing in mammalian cells. Curr Opin Cell Biol 2005, 17:309–315
27. Mellerio JE, Dunnill MG, Allison W, Ashton GH, Christiano AM, Uitto J, Eady RA, McGrath JA: Recurrent mutations in the type VII collagen gene (COL7A1) in patients with recessive dystrophic epidermolysis bullosa. J Invest Dermatol 1997, 109:246–249
28. Pulkkinen L, Uitto J: Mutation analysis and molecular genetics of epidermolysis bullosa. Matrix Biol 1999, 18:29–42
29. Gardella R, Castiglia D, Posteraro P, Bernardini S, Zoppi N, Paradisi M, Tadini G, Barlati S, McGrath JA, Zambruno G, Colombi M: Genotype-phenotype correlation in Italian patients with dystrophic epidermolysis bullosa. J Invest Dermatol 2002, 119:1456–1462
30. Kern JS, Kohlhase J, Bruckner-Tuderman L, Has C: Expanding the COL7A1 mutation database: novel and recurrent mutations and unusual genotype-phenotype constellations in 41 patients with dystrophic epidermolysis bullosa. J Invest Dermatol 2006, 126:1006–1012
31. Varki R, Sadowski S, Uitto J, Pfendner E: Epidermolysis bullosa. II. Type VII collagen mutations and phenotype-genotype correlations in the dystrophic subtypes. J Med Genet 2007, 44:181–192

Correspondence

Scleroedema adultorum associated with sarcoidosis

doi: 10.1111/j.1365-2230.2009.03423.x

Sarcoidosis is a systemic granulomatous disease of unknown aetiology that displays a wide variety of skin features including maculopapules, nodules, plaques, subcutaneous nodules, infiltrative scars, and lupus pernio.[1] We report a case of sarcoidosis with subcutaneous induration of the neck.

A 62-year-old Japanese man presented with a 6-month history of asymptomatic, firm indurations on the neck. He had first noticed these skin lesions after bilateral symmetrical hilar lymph-node enlargement was found during routine chest radiography. Transbronchial biopsies resulted in the histological identification of non-caseating granulomas compatible with sarcoidosis. The patient had no history of diabetes mellitus or preceding infection.

On physical examination, symmetrical, hard, nonpitting indurations of the skin were found on the posterior neck (Fig. 1a). The patient's general health was good.

Results of routine laboratory studies including angiotensin-converting enzyme and tuberculin response gave normal results, and there was no evidence of monoclonal proteinaemia. Computed tomography scans showed bilateral hilar lymphadenopathy but there was no other lymphadenopathy noted.

Histological examination of skin-biopsy specimens taken from the posterior neck revealed swelling of the dermal collagen bundles without increase in fibroblast numbers, and the subcutaneous fat had been replaced by collagen fibres (Fig. 1b). A diagnosis of SA was made. Treatment was started with steroid ointment or 9 months, but without evident improvement.

SA is a rare disorder of unknown cause, but often complicates diabetes mellitus. In such cases, the lesions are usually limited to neck and upper back, and tend to be persistent.[2] In contrast, in SA not associated with diabetes mellitus, the lesions often spread to the face, trunk and upper arms, but may spontaneously subside.[3,4] However, in spite of no obvious association with diabetes mellitus, our patient had intractable induration distributed over a localized area. Interestingly, in this case, development of the skin lesion was coincidental with the diagnosis of sarcoidosis. The clinical appearance was indicative of scleroedema. There have been no previous reports of any association between SA and sarcoidosis. Therefore, we first suspected a subcutaneous form of sarcoidosis rather than scleroedema. However, the histopathological findings confirmed a diagnosis of scleroedema.

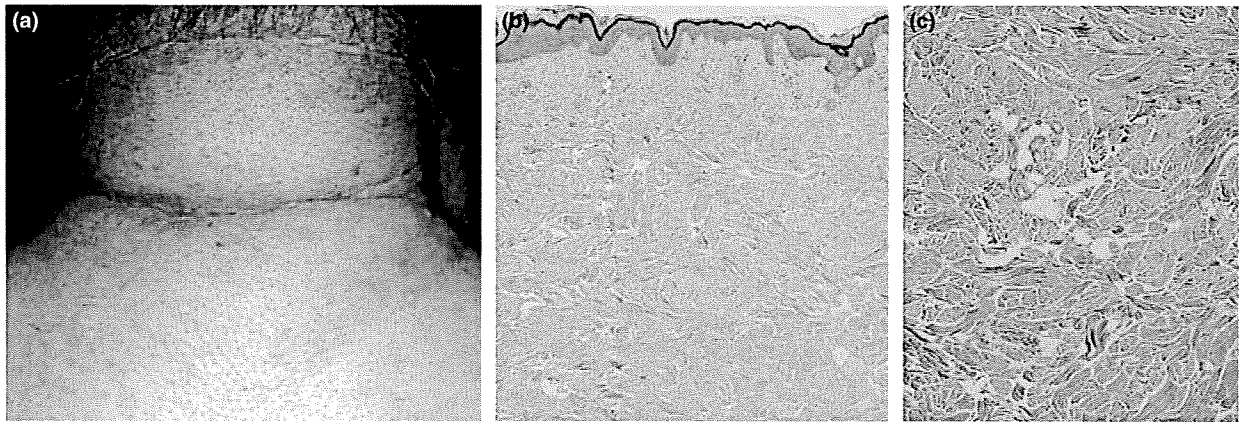

Figure 1 (a) Symmetrical, hard, nonpitting induration on the posterior side of the neck; (b) inflammatory cell infiltration in the upper dermis and swelling of collagen bundles in the lower dermis; (c) swelling of the dermal collagen bundles without any increase in fibroblast numbers, and the replacing of subcutaneous fatty tissues by collagen fibres.